



저작자표시-비영리-변경금지 2.0 대한민국

이용자는 아래의 조건을 따르는 경우에 한하여 자유롭게

- 이 저작물을 복제, 배포, 전송, 전시, 공연 및 방송할 수 있습니다.

다음과 같은 조건을 따라야 합니다:



저작자표시. 귀하는 원저작자를 표시하여야 합니다.



비영리. 귀하는 이 저작물을 영리 목적으로 이용할 수 없습니다.



변경금지. 귀하는 이 저작물을 개작, 변형 또는 가공할 수 없습니다.

- 귀하는, 이 저작물의 재이용이나 배포의 경우, 이 저작물에 적용된 이용허락조건을 명확하게 나타내어야 합니다.
- 저작권자로부터 별도의 허가를 받으면 이러한 조건들은 적용되지 않습니다.

저작권법에 따른 이용자의 권리는 위의 내용에 의하여 영향을 받지 않습니다.

이것은 [이용허락규약\(Legal Code\)](#)을 이해하기 쉽게 요약한 것입니다.

[Disclaimer](#)

Master's Thesis

Study on Si-Conducting Polymer Core-Shell Anodes
for Lithium-Ion Batteries

Sunghee Shin

Department of Energy Engineering
(Battery Science and Technology)

Graduate School of UNIST

2018

Study on Si-conducting Polymer Core-Shell Anodes for Lithium-Ion Batteries

Sunghee Shin

Department of Energy Engineering
(Battery Science and Technology)

Graduate School of UNIST

Study on Si-Conducting Polymer Core-Shell Anodes for Lithium-Ion Batteries

A thesis/dissertation
submitted to the Graduate School of UNIST
in partial fulfillment of the
requirements for the degree of
Master of Science

Sunghee Shin

06. 01. 2018.

Approved by

Advisor
Soojin Park

Study on Si-Conducting Polymer Core-Shell Anodes for Lithium-Ion Batteries

Sunghee Shin

This certifies that the thesis/dissertation of Sunghee Shin is approved.

06. 01. 2018.

signature

Advisor: Soojin Park

signature

Nam-Soon Choi

signature

Seok Ju Kang

Contents

List of Figures-----	7
List of Tables-----	11
Abstract-----	12
Chapter 1. Introduction-----	9
1.1. Overview of Global Energy-----	9
References-----	13
1.2. Lithium-Ion Batteries-----	14
1.2.1. Basic Principles of Lithium-Ion Batteries-----	14
1.2.2. Components of Lithium-Ion Batteries-----	16
1.2.3. Cathode materials-----	19
1.2.4. Anode materials-----	23
1.2.5. Separators-----	25
1.2.6. Electrolytes-----	28
References-----	31
1.3. Conducting Polymers-----	36
1.3.1. Introduction of Conducting Polymers-----	36
1.3.2. Basic Principles of Conducting Polymers-----	40
1.3.3. Polymerization mechanisms-----	43
1.3.4. Applications of Conducting Polymers-----	47
References-----	48
Chapter 2. Study on Si-conducting polymer core-shell anodes for lithium-ion batteries-----	51
2.1. Introduction-----	51
2.2. Experimental Section-----	52
2.2.1. Synthesis of 2D Silicon flake (Si flake) -----	52
2.2.2. Synthesis of 2D Si flake @ Polypyrrole (PPy) -----	52
2.2.3. Synthesis of 2D Si flake @ SO ₃ doped polyaniline (PANI) -----	52
2.2.4. Characterization-----	53

2.2.5. Electrochemical measurements-----	53
2.3. Results and Discussion-----	54
2.4. Conclusion-----	62
References-----	63

List of Figures

Figure 1.1.1. Schematic figures of annual change of consumption and production of oil market in 2015 and 2016. (Mb/d)

Figure 1.1.2. Schematic figures of annual change of China coal production growth (%) and China coal prices (5500 kcal/kg) in 2015 and 2016.

Figure 1.1.3. Schematic figures of annual change of supply and demand of LNG in 2015 and 2016. (unit : bcm)

Figure 1.1.4. Classification of electrical energy storage systems according to energy form (Fraunhofer ISE)

Figure 1.2.1. Schematic showing a configuration of rechargeable Li-ion batteries.

Figure 1.2.2. Five performance criteria as measures to evaluate cathode materials. The values of each criterion were indicated for four different cathode materials. (a) LCO = LiCoO_2 , layered, (b) NMC = $\text{LiNi}_x\text{Mn}_y\text{Co}_z\text{O}_2$, layered, NCA = $\text{LiNi}_{1-y-z}\text{Co}_y\text{Al}_z\text{O}_2$, layered, (c) LMO = LiMn_2O_4 spinel, and (d) LFP = LiFePO_4 olivine.

Figure 1.3.1. Comparison of the conductivities of doped conducting polymers with those of conventional conductors.

Figure 1.3.2. Molecular structures of some representative conducting polymers

Figure 1.3.3. A simplified schematic of a conjugated backbone: a chain containing alternating single and double bonds.

Figure 1.3.4. A simplified explanation of the electrical conductivity of conducting polymers. (A) The dopant removes or adds an electron from/to the polymer chain, creating a delocalized charge. (B) It is energetically favorable to localize this charge and surround it with a local distortion of the crystal lattice. (C) A charge surrounded by a distortion is known as a polaron (a radical ion associated with a lattice distortion). (D) The polaron can travel along the polymer chain, allowing it to conduct electricity.

Figure 1.3.5. Schematic comparing the chemical, electrochemical, and photopolymerization mechanisms. V: variables, C: cost effectiveness, M: morphology control, T: time of reaction, and R: resulting purity of the materials.

Figure 1.3.6. Schematic of nanohybrid synthesis methods. Each mechanism has been evaluated in terms of variables (V), in which a low value means there are many key variables in the synthesis process; cost (C), in which a low value corresponds to high cost; morphology control (M); time required (T); scalability (S); and purity (P) of products.

Figure 2.3.1. SEM images of 2D Si flake (a)) and 2D Si flake@PPy. (b) to c)).

Figure 2.3.2. EDS data of a) 2D Si flake and b) 2D Si flake@PPy

Figure 2.3.3. XRD patterns of a) 2D Si flake and b) 2D Si flake@conducting polymers.

Figure 2.3.4. SEM images of 2D Si flake@SO₃ doped PANI in an a) low magnitude, and b) high magnitude. c) is a high magnitude of PANI hydrochloric salt, and d) is an EDS data of the 2D Si flake@SO₃ doped PANI.

Figure 2.3.5. TEM images of 2D Si flake@PPy (a) to b)) and 2D Si flake@SO₃ doped PANI (c) to d)).

Figure 2.3.6. Electrochemical performance of Si@PPy and Si@SO₃-doped PANI electrodes. A) and b) are first cycle of each material. First cycle voltage profiles obtained at the 0.1C between 0.005V to 1.5V. Cycle performance of Si@PPy and Si@SO₃-doped PANI at rate of 0.5C.

Figure 2.3.7. Cross-sectional SEM images of electrode before and after cycle. a) as-synthesized 2D Si flake electrode before cycle and b) is after 50 cycles of 2D Si flake electrode. c) is 2D Si flake @ SO₃ doped PANI electrode before cycle and d) is after 50 cycles of 2D Si flake @ SO₃ doped PANI electrode.

List of tables

Table 1.2.1. Components and examples of materials for lithium-ion batteries.

Table 1.2.2. Electrochemical characteristics of various types of cathode materials.

Table 1.2.3. electrochemical characteristics of various types of anode materials.

Table 1.2.4. General requirements for separators

Table 1.2.5. Commercial separator properties

Table 1.2.6. Representative cyclic and linear carbonates as electrolyte solvents and their characteristics.

Table 1.2.7. Comparison of lithium salt characteristics

Table 1.3.1. The conductivity, stability and processability of a number of conducting polymers.

Abstract

Conducting polymer is an eccentric polymer having flexibility, high electric conductivity, and easiness to synthesis. Through these advantages, conducting polymer has widely range of use: supercapacitors, batteries, electrochromic devices, solar cells, sensors, and biomedical applications.

Lithium-ion batteries (LIBs) are considered as a good candidate for energy applications because of their response time, high cycle efficiencies, and so on.

To make high capacity batteries, developing anode material is an inevitable work. Above all, silicon-based anode materials are rising stars for their high capacity, abundance in earth crust, and eco-friendly. However, severe critical issues like volume expansion remain.

In this paper, we studied on 2D Si flake @ PPy synthesized by vapor phase polymerization and 2D Si flake @ SO₃ doped PANI to refine the problem of Si anode.

In the case of 2D Si flake @ PPy, initial coulombic efficiency (ICE) was 85%, because, overoxidation occurs during synthesis. On the other hand, in the case of SO₃ doped polyaniline (PANI), it shows 98.4%, 13.4% higher than PPy coated Si. 2D Si flake @ PPy and 2D Si flake @ SO₃ doped PANI were synthesized to improve the disadvantages of Si anode. 2D Si flake @ PPy adopted vapor phase polymerization to simplify the coating method, but, it was hard to gain uniformly coated sample, and overoxidation reaction occurs through the reaction. Spring from overoxidation reaction, it increased Li⁺ intercalation but deintercalation didn't keep up with the amount of intercalated Li⁺. Overoxidation led the drop of the initial coulombic efficiency. On the other hand, 2D Si flake @ SO₃ doped PANI displayed uniformly coated Si anode and prevented overoxidation through dissolving and reconstruction in NMP solution. Moreover, 2D Si flake @ SO₃ doped PANI exhibited high initial coulombic efficiency, good cycling performance, and suppressed expansion.

Chapter 1. Introduction

1.1. Overview of Global Energy

According to BP's Statistical Review of World Energy 2017, global primary energy consumption increased by just 1% in 2016, following growth of 0.9% in 2015 and 1% in 2014. This compares with growth of primary energy consumption as well below the 10-year average of 1.8%.

2015 was a year of dashed adjustment for oil: strong growth in Organization of Petroleum Exporting Countries (OPEC) production outweighed the responses of both demand and non-OPEC production to lower prices (See Figure 1.1.1.). In contrast, 2016 was a year of adjustment for the oil market, with oil demand again increasing sturdily and production growing by less than a quarter (0.4 Mb/d) of that seen in 2015. On the other hand, 2016 saw a 1.2% drop in output from 2015, due to a drop output from OPEC and Non-OPEC. As shown in Figure 1.1., Non-OPEC supplied 1.3% in 2015, but it supplied -0.8% in 2016.

Oil is not the only one that is inconsistent with supply and demand. For instance, China's coal production fell by 7.9% in 2016 (See Figure 1.1.2.). It affected the increase in coal prices. For natural gas, annual change of supplying the natural gas is more than 5 times bigger than 5-year average annual supply. Not only annual change of supplying, annual change of demand is robustly increased than 5-year average annual demand (See Figure 1.1.3.).¹

It means that production of fossil fuel doesn't satisfy the demand. Therefore, our society is facing the depletion of fossil fuels and the rising demand for energy sources increases the need for the development of next-generation energy sources.

For this reason, the development and application of storage devices is of interest in both industry and research. Electrical Energy Storage (EES) refers to a process of converting electrical energy from a power network into a form that can be stored for converting back to electrical energy when needed.²⁻⁴ Such a process enables electricity to be produced at times of either low demand, low generation cost or from intermittent energy sources and to be used at times of high demand, high generation cost or when no other generation means is available.²⁻⁶

A widely-used approach for classifying EES systems is the determination according to a form of energy used. In Figure 1.4., EES systems are classified into mechanical, electrochemical, chemical, electrical and thermal energy storage systems. In electrical section, there are various types of batteries. Most of them are technically commercialized. Lead acid, NiCd/NiMH, Li-ion, metal air, sodium sulphur and sodium nickel chloride are included in secondary battery types and redox flow, and hybrid flow batteries are included in flow batteries.⁷

Among them, lithium-ion batteries (LIBs) are one of the most widely used secondary battery

systems. LIBs are considered as a good candidate for applications where the response time, small dimension and/or weight of equipment are important (milliseconds response time, $\sim 1500\text{--}10,000$ W/L, $\sim 75\text{--}200$ W h/kg, $\sim 150\text{--}2000$ W/kg). LIBs also have high cycle efficiencies, up to $\sim 97\%$.^{8,10} Xing Luo et al. mentioned that “The main drawbacks are that the cycle DoD can affect the Li-ion battery’s lifetime and the battery pack to manage its operation, which increases its overall cost.”¹¹



Figure 1.1.1. Schematic figures of annual change of consumption and production of oil market in 2015 and 2016. (Mb/d)¹

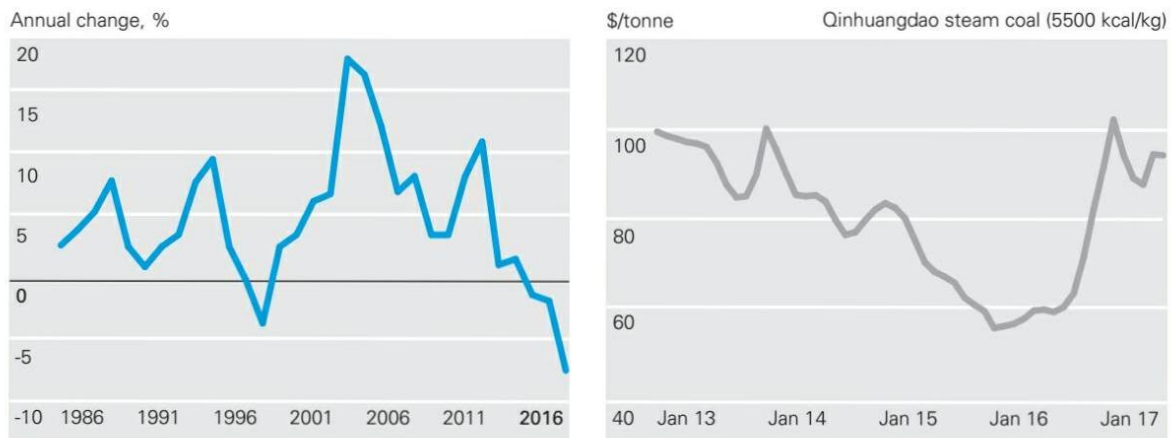
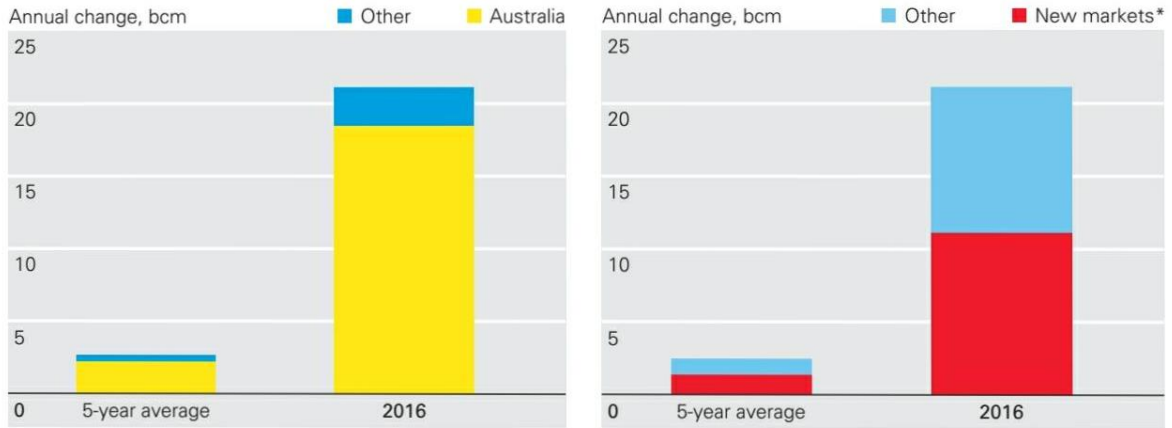


Figure 1.1.2. Schematic figures of annual change of China coal production growth (%) and China coal prices (5500 kcal/kg) in 2015 and 2016.¹



*Includes Egypt, Pakistan, Poland, Jamaica, Colombia and Lithuania

Figure 1.1.3. Schematic figures of annual change of supply and demand of LNG in 2015 and 2016. (unit : bcm)¹

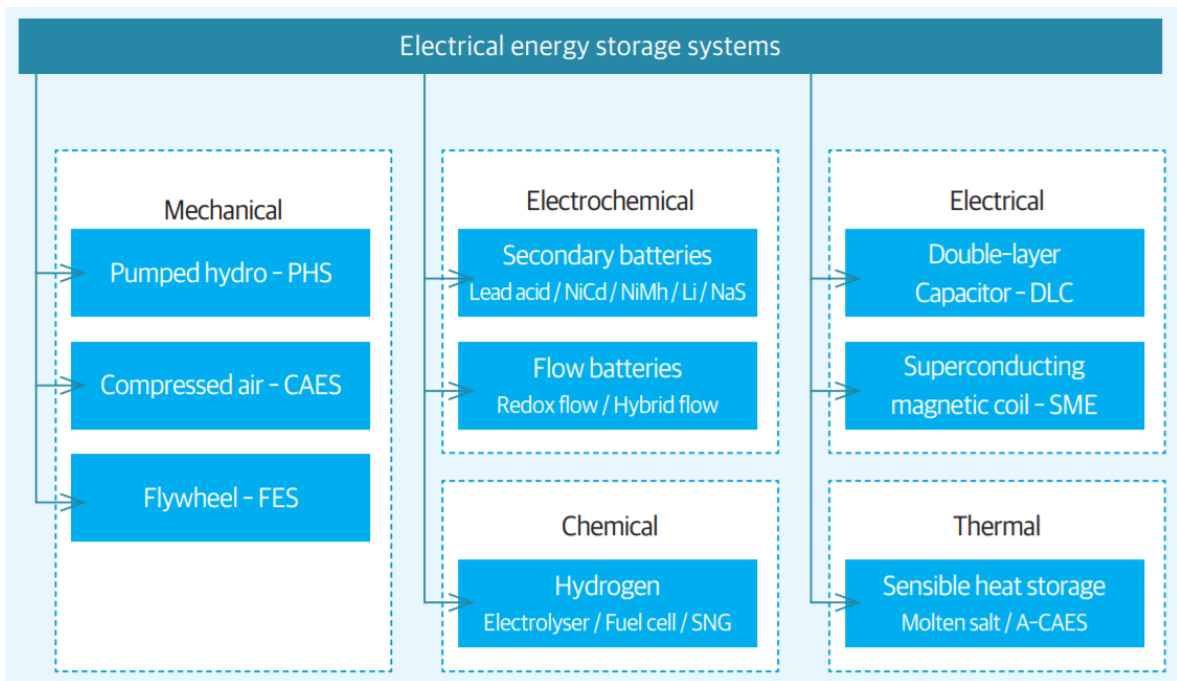


Figure 1.1.4. Classification of electrical energy storage systems according to energy form (Fraunhofer ISE)⁷

References

1. BP's Statistical Review of World Energy 2017
<<https://www.bp.com/content/dam/bp/en/corporate/pdf/energy-economics/statistical-review-2017/bp-statistical-review-of-world-energy-2017-full-report.pdf>>
2. McLaren FR, Cairns EJ. Energy storage. *Ann Rev Energy* 1989;14:241–71.
3. Baker JN, Collinson A. Electrical energy storage at the turn of the millennium. *Power Eng J* 1999;6:107–12.
4. Dti Report. Status of electrical energy storage systems. DG/DTI/00050/00/00, URN NUMBER 04/1878, UK Department of Trade and Industry; 2004, p. 1–24.
5. Australian Greenhouse Office. Advanced electricity storage technologies programme. ISBN: 1 921120 37 1, Australian Greenhouse Office; 2005, p. 1–35.
6. Walawalkar R, Apt J, Mancini R. Economics of electric energy storage for energy arbitrage and regulation. *Energy Policy* 2007; 5:2558–68.
7. International Electrochemical Commission White paper, Electrical Energy Storage
<<http://www.iec.ch/whitepaper/pdf/iecWP-energystorage-LR-en.pdf>>
8. Review of electrical energy storage technologies and systems and of their potential for the UK. Dti Report. DG/DTI/00055/00/00. UK Department of Trade and Industry; 2004
9. Electrical energy storage: white paper. Technical report. Prepared by electrical energy storage project team. International Electrotechnical Commission (IEC), Published December 2011.
<<http://www.iec.ch/whitepaper/pdf/iecWP-energystorage-LR-en.pdf>> [accessed 15.05.14].
10. Hadjipaschalis I, Poullikkas A, Efthimiou V. Overview of current and future energy storage technologies for electric power applications. *Renew Sust Energy Rev* 2009; 13:1513–22.
11. Xing Luo, Jihong Wang et al., *Applied Energy* 137 (2015) 511–536

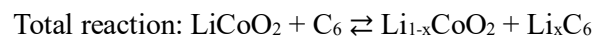
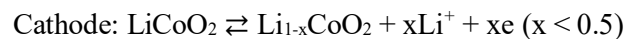
1.2. Lithium-Ion Batteries

1.2.1. Basic Principles of Lithium-Ion Batteries

Depleting fossil fuels and increasing the usage of energy sources request next-generation energy devices to overcome these encountered issues. Lithium ion batteries (LIBs), which have high energy density, become one of the powerful alternatives.

LIBs have the same construction as conventional batteries. LIBs consist of cathode, anode, separator, and electrolytes. The similarities between LIBs and conventional batteries cover reduction-oxidation (redox) reactions at the interfaces between the electrolyte and electrodes, accompanied by the diffusion of ions in the electrolyte. However, the differences between conventional batteries and LIBs are notable. In typical galvanic batteries, the redox reactions proceed simultaneously with the fading or advancing of electrode surfaces, but not accompanied by either solid-state mass diffusion in the electrodes or a change in the chemical composition and local atomic environment.² On the other hand, the heterogeneous redox reactions in LIBs are similar with electrolytic cells. They accompanied by the solid-state mass diffusion as well as a volume expansion. LIBs are one of the rechargeable batteries, in which Li ions move from cathode materials to anode materials as shown in Figure 1.2.1.

The following equations demonstrate the chemical reactions during the discharge and charge at anode and cathode of commercial LIB.³



Driving force of LIBs is a potential difference between anode and cathode. To increase energy density, cathode materials should have higher potential and anode should have lower potential. The amounts of ions which inserts into electrodes determines a specific capacity of electrical storage devices. It indicates that Li ions and materials are main factors that can affect the amount of electric energy to be stored.⁴

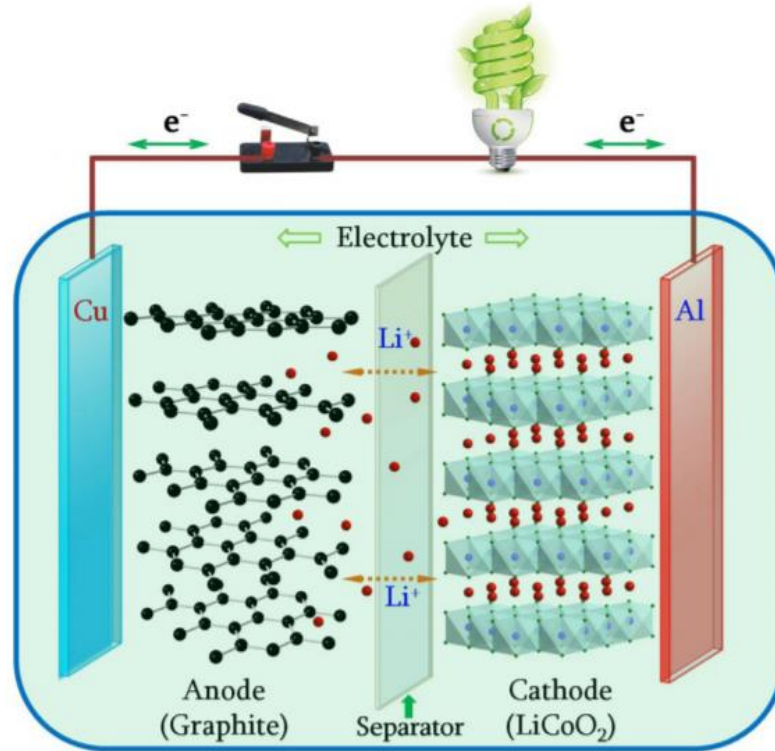


Figure 1.2.1. Schematic showing a configuration of rechargeable Li-ion batteries.¹

1.2.2. Components of Lithium-Ion Batteries

As stated above, the LIBs are composed of cathode, separator, anode, and electrolyte (See Table 1.2.1.). Commercial LIBs employed a graphite anode, an electrolyte based on a lithium salt and a carbonate solvent, and a LiCoO₂ cathode, resulting in a gravimetric energy density of about 190 Wh/kg.⁵ The conventional graphite/LiCoO₂ cell has several intrinsic limitations, including (i) relatively limited intercalation ability of graphite (i.e., about 0.17 moles of Li per mole of carbon); (ii) high cost and environmental issues posed by the use of Co; (iii) low thermal stability of Li_{1-x}CoO₂ (x < 0.5) phase formed during charge process.^{6,7} Although various substances and components have been explored to overcome these limitations of conventional cell, the basic design of LIB is still the same as these cells that the Sony has commercialized two decades ago.

In case of cathode materials, each lithium ion escaped from the center of layers during discharge state. Cathode materials are classified into four types depending on their structures as follows: (1) layered structures (e.g. LiTiS₂, LiCoO₂, LiNiO₂, LiMnO₂, LiNi_{0.33}Co_{0.33}O₂, LiNi_{0.8}Co_{0.15}Al_{0.05}O₂ and LiMnO₃), (2) spinel structures (e.g. LiMn₂O₄, and LiCo₂O₄), (3) olivine structures (e.g. LiFePO₄, LiMnPO₄, and LiCoPO₄), and (4) tavorite structures (e.g. LiFeSO₄F, and LiVPO₄F). Layered-structured cathodes, among which the most widely known as LiCoO₂ (LCO), currently represent the cathode materials for use in combination with a graphite anode.^{6,7}

Meanwhile, cathode materials release lithium ions from their lattice structure during lithiation process, anode materials stored lithium ions into their lattice and they supply large electromotive force through the charge-discharge reaction. Anode materials are easily sorted into two types in Table 1. 2.1; graphite-based or non-graphitic-based carbon. Graphite-based anode materials (e.g. graphite, hard carbon, and soft carbon) have been widely used for their long cycle life, abundance and relatively inexpensive. However, low energy density (372 mAh/g), and safety issues related to lithium deposition are critical weak points. To improve these problems, metalloids (e.g. silicon (Si), germanium (Ge), tin (Sn), antimony (Sb), bismuth (Bi), and so on.)⁸⁻¹⁰, and metal oxides (e.g. tin oxide, copper oxide, iron oxide, ruthenium oxide, manganese oxide, silicon oxide, lithium titanium oxide, and so on.) are included in non-graphite based materials, are receiving much attention these days.

When two electrodes with different electric potential create a potential difference in the electrolyte, separator acts as a “shield” to prevent physical contact of electrodes in a battery system. Unlike cathode and anode, separator placed between them is an insulator. Although the separator doesn't involve any reactions in any cell reactions, its structure and properties play an important role in determining battery performance, including cycle life, cell safety, energy density, and power density, through influencing the cell kinetics.¹² Polyethylene (PE), polypropylene (PP), and polyvinylidene

fluoride (PVdF) are typical separators. Moreover, ceramic materials can be introduced to the separator. However, when they have a poor wettability in electrolytes, low thermal stability or low chemical stability, they hindered the high cell performance. For the development of future Li-ion batteries for high-temperature applications, inorganic membranes as separators are highly attractive. The electrolytes consist of lithium salt and non-aqueous organic solvent with electrochemical, thermal, and chemical stabilities in the range of working voltage.¹¹

Each component will be described more detail in following pages.

Table 1.2.1. Components and examples of materials for lithium-ion batteries.

Component		Materials
Cathode		Layered structure LiTiS ₂ , LiCoO ₂ , LiNiO ₂ , LiMnO ₂ , LiNi _{0.33} Co _{0.33} O ₂ , LiNi _{0.8} Co _{0.15} Al _{0.05} O ₂ , LiMnO ₃
		Spinel structure LiMn ₂ O ₄ , LiCo ₂ O ₄
		Olivine structures LiFePO ₄ , LiMnPO ₄ , LiCoPO ₄
		Tavorite structure LiFeSO ₄ F, LiVPO ₄ F
Anode		Graphite-based materials Graphite, hard carbon, soft carbon
		Non graphite-based materials Metalloids, metal oxides
Separator		Polymer Polyethylene (PE), polypropylene (PP), Polyvinylidene fluoride (PVdF)
Electrolyte	Lithium salt	Organic and inorganic lithium compound LiPF ₆ , LiBF ₄ , LiAsF ₆ , LiClO ₄ , LiCF ₃ SO ₃ , Li(CF ₃ SO ₂) ₂ N
	Electrolyte solvent	Nonaqueous organic solvent Ethylene carbonate (EC), Propylene carbonate (PC), Dimethyl carbonate (DMC), Diethyl carbonate (DEC), Ethylmethyl carbonate (EMC)

1.2.3. Cathode Materials

For high energy, high power and long cycle life, cathode material is a critical core component of LIBs. That's why the rush in the industry to develop the next generation LIBs, which have higher power and more energy densities, has normally focused on the investigation of new and higher performing cathode materials.

There are several things that should be qualified to characterize the cathode materials: 1) To intercalate a large amount of lithium ions, cathode materials should display reversible behavior and a flat potential so as to enhance energy efficiency during charge/discharge process. 2) They should be light and densely packed to allow high capacity per weight or volume, and they have high electrical and ionic conductivities for high power. 3) High cycle efficiency must be maintained. 4) Such phase transitions should not occur in cathode materials during charge/discharge although cycle life is shortened by irreversible phase transitions of the crystal structure. 5) They should have electrochemical and thermal stability to head reactions off with the electrolyte. 6) The particles of cathode materials must be globular with a narrow grain size distribution, so that the aluminum current collector remains intact when making electrodes.¹⁴ 7) They should be low cost and be environmentally benign.

As shown in Table 1.2.2., cathode materials are classified into four types. The first contains layered compounds with an anion close-packed or almost close-packed lattice in which alternate layers between anion sheets occupied by a redox-active transition metal and lithium then inserts itself into the essentially empty remaining layers. This group is exemplified by first LiTiS_2 , and followed by LiCoO_2 , LiNiO_2 , LiMnO_2 , and so on. Spinel structures may be considered as a special case where transition-metal cations are ordered in all the layers. The materials in the second group have more open structures, like many of vanadium oxides, tunnel compounds of manganese dioxide, and most recently transition-metal phosphates, such as the olivine LiFePO_4 . The first group, because of their more compact lattices, will have an inherent advantage in energy stored per unit of volume, but some in the second group, such as LiFePO_4 , are potentially much lower cost.

Conventional cathode materials generally fall into two types. LiCoO_2 adopts a layered, rhombohedral structure with two-dimensional Li-ion diffusion parallel to the planar sheets of metal cations. On the other hand, another material such as LiMn_2O_4 , adopt the spinel structure and allow Li ions diffusion in three dimensions.¹³

Materials containing polyatomic phosphate(PO_4)³⁻ anions tend to have higher thermal stability than oxides with comparable voltages, but these large and heavy anions adversely affect specific capacity. One way to compensate for this loss of capacity would be to develop a material that contains a polyatomic anion and is capable of reversibly inserting two lithium ions per redox-active metal ion.

Recent studies indicate that materials with a structure similar to $\text{LiFe}(\text{PO}_4)(\text{OH})$ (tavorite) might be able to achieve this goal.

Table 1.2.2. Electrochemical characteristics of various types of cathode materials.

Crystal structure	Compound	Specific capacity (mAh/g)	Volumetric capacity (mAh/cm ³)	Voltage (V)
Layered	LiTiS ₂	225	697	1.9
	LiCoO ₂	274	1363	3.8
	LiNiO ₂	275	1280	3.8
	LiMnO ₂	285	1148	3.3
	LiNi _{0.33} Mn _{0.33} Co _{0.33} O ₂	280	1333	3.7
	LiNi _{0.8} Co _{0.15} Al _{0.05} O ₂	279	1284	3.7
Spinel	Li ₂ MnO ₃	458	1708	3.8
	LiMn ₂ O ₄	148	596	4.1
	LiCo ₂ O ₄	142	704	4.0
Olivine	LiFePO ₄	170	589	3.4
	LiMnPO ₄	171	567	3.8
	LiCoPO ₄	167	510	4.2
Tavorite	LiFeSO ₄ F	151	487	3.7
	LiVPO ₄ F	156	484	4.2

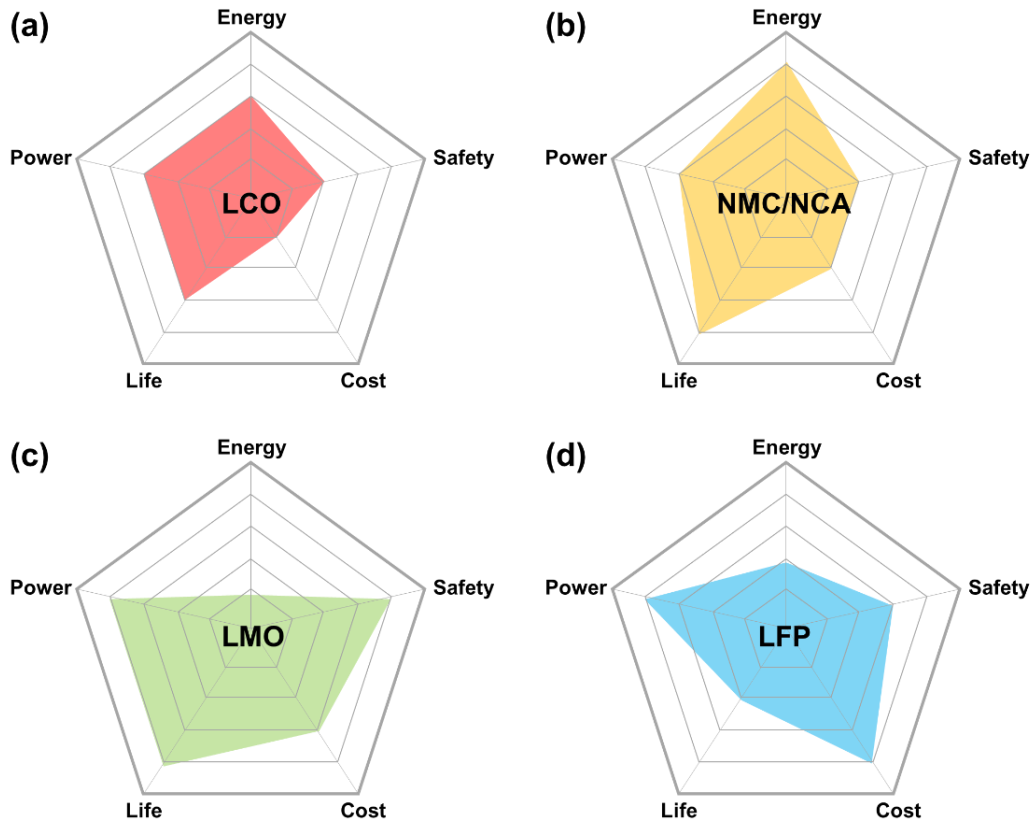


Figure 1.2.2. Five performance criteria as measures to evaluate cathode materials. The values of each criterion were indicated for four different cathode materials. (a) LCO = LiCoO_2 , layered, (b) NMC = $\text{LiNi}_x\text{Mn}_y\text{Co}_z\text{O}_2$, layered, NCA = $\text{LiNi}_{1-y-z}\text{Co}_y\text{Al}_z\text{O}_2$, layered, (c) LMO = LiMn_2O_4 spinel, and (d) LFP = LiFePO_4 olivine.^{15, 16}

1.2.4. Anode Materials

Park et al. mentioned that the requirements of anode materials are mentioned: “1) They should have a low potential corresponding to a standard electrode and provide a high cell voltage with the cathode. The potential relating to electrochemical reactions must be a close approximation with electrochemical potential of lithium metal. 2) No significant change in the crystal structure should occur during reactions with lithium ions. Change in structure leads to the accumulation of crystal strain and hinders the reversibility of electrochemical reactions, thus resulting in poor cycle life characteristics. 3) They should engage in highly reversible reactions with lithium ions. 4) Fast diffusivity of lithium ions is required within the active electrode material at the anode since this is particularly important to realize cell performance. 5) High electronic conductivity is necessary to facilitate the movement of electrons during electrochemical reactions. 6) They should be sufficiently dense so as to obtain a high electrode density. This is an important design factor that is considered to enhance battery energy. 7) Materials should store a large amount of charge (coulomb) per unit mass.”¹⁷

Other important factors that determine energy density and power are specific surface area, tap density, particle size, and distribution. Because the anode has a large specific capacity per unit mass, it is more difficult to intercalate or deintercalated lithium ions in comparison with the cathode. As such, the design of the anode should take into account the fast movement of lithium ions in order to enhance the performance of Li batteries.

Among anode materials, anode materials based on graphite is commercially used due to their excellent cycling performance. However, graphite anode limits to increasing demand on energy density, operation reliability and system integration arising from portable electronic devices, electric vehicles, and energy storage applications. Moreover, graphite anodes exhibit only a moderate intrinsic specific capacity (372 mA h/g) and serious safety issue concerns due to lithium plating and further formation of lithium dendrites. To overlap these matters, there are various types of anode materials that can be classified according to their reaction with lithium ions as follows (Table 1.2.3.): 1) Formation of metal alloy (group IV elements (metalloids); silicon, tin, germanium, aluminum, and antimony, etc.),¹⁸⁻²⁰ and 2) Conversion reaction with lithium (transition metal oxides; Fe₂O₃, Fe₃O₄, CuO, Cu₂O, NiO, Ni₂O, MnO, MnO₂, etc.)²¹

Table 1.2.3. electrochemical characteristics of various types of anode materials.

Materials	Li	C	Li₄Ti₅O₁₂	Si	Sn	Sb	Al	Mg	Bi
Density (g/cm ³)	0.53	2.25	3.5	2.33	7.29	6.7	2.7	1.3	9.78
Lithiated phase	Li	LiC ₆	Li ₇ Ti ₅ O ₁₂	Li _{4.4} Si	Li _{4.4} Sn	Li ₃ Sb	LiAl	Li ₃ Mg	Li ₃ Bi
Theoretical specific capacity (mAh/g)	3862	372	175	4200	994	660	993	3350	385
Theoretical charge density (mAh/cm ³)	2047	837	613	9786	7246	4422	2681	4355	3765
Volume change (%)	100	12	1	320	260	200	96	100	215
Potential vs. Li (V)	0	0.05	1.6	0.4	0.6	0.9	0.3	0.1	0.8

1.2.5. Separators

Each lithium-ion battery consists of an anode, a cathode, and a separator. The separator properties play a critical role in obtaining optimum cell performance and the inherent safety of the cell. The separator membrane separates two electrodes and serves as “aisle” for the lithium-ion transport between two electrodes to control the number of lithium ions and their mobility. Porous structure of the separator is filled with liquid electrolyte (lithium salt dissolved in a mixture of one or more solvents). When a charge process occurs, an external electrical power source injects electrons into the anode. At the same time, the cathode gives up some of its lithium ions, which move through the electrolyte to the anode and remain there. During this process, electricity is stored in the battery in the form of chemical energy. On the other hand, during a discharge process, lithium ions move back across the electrolyte to the cathode, enabling the release of electrons to the outer circuit to perform the electrical work. General requirements of separator are followed in Table 1.2.4.

As shown in Table 1.2.4., separators must be chemically and electrochemically stable to resist degradation or dissolution the electrolyte and electrode materials in battery system for cell longevity. These porous membranes should have uniform pore distribution and be inert under battery system. They should wet quickly and completely in electrolyte, not swell. While they wet easily in the electrolyte, they should not curl up and lay flat to separate between two electrodes. Furthermore, they should more than 5% of contraction after 60 min at 90°C to effectively shut down the battery at elevated temperatures. Thickness of the ideal separators are also important because they are inactive materials in system. Recommended thickness is 20-25 μm .

Through these requirements, there are various kinds of attempts reported by using polyolefin microporous films (PE, PP), polyvinylidene fluoride (PVdF)²⁴, inorganic nanoparticle (SiO₂, TiO₂, Al₂O₃, ZrO₂, etc.) coated polymer.²⁵

Most commercially available non-aqueous lithium-ion separators designed for small batteries (<3 Ah) are single layer (Entek (PE, Teklon) and Tonen (PE, Exxon), see Table 1.2.5.), or multilayer (2325 (PP-PE-PP, Celgard)) polymer sheets typically made of polyolefins, which have transition temperatures of 135°C (PE) and 165°C (PP), respectively, but are somewhat dependent on molecular weight. Their porosities below or similar with ideal porosity requirements.

Table 1.2.4. General requirements for separators²²

Parameter	Requirement
Chemical and electrochemical stabilities	Stable for a long period of time
Wettability	Wet out quickly and completely
Mechanical property	> 1000kng/cm (98.06 MPa)
Thickness	20-25 μ m
Pore size	<1 μ m
Porosity	40-60%
Permeability (Gurley)	<0.025 s/ μ m
Dimensional stability	No curl up and lay flat
Thermal stability	<5% shrinkage after 60 min at 90°C
Shutdown	Effectively shut down the battery at elevated temperatures

Table 1.2.5. Commercial separator properties²³

Separator manufacturers [a]	ASAHI	TORAY	CELGARD	UBE	ENTEK
Product	HIPORE	SETELA	Celgard	UPORE	Teklon
Thickness (μm)	≥25	7-25	ML PP: 16-25ML PE: 16-20 TL PP/PE/PP: 12-38	-	25
Single/multilayer	SL	SL	SL/ML	SL	SL
Composition [b]	PE	PE	SL: PP, PE ML: PP/PE/PP	PP, PE	PE
Process	Wet-extruded	Wet-extruded	Dry-extruded	Dry-extruded	Wet-extruded

[a] Separator specifications are found on data sheets for each product. [b] PE : polyethylene, PP: polypropylene [c] SL : single-layer, TL : trilayer

1.2.6. Electrolytes

Liquid electrolytes, which composed of organic solvents, lithium salts, and additives, are normally used in LIB system. These act as a way for the transport of lithium ions.

Electrolytes could be attributed to three distinct, but interdependent factors: (1) Their components (especially solvents) are more sensitive to operate potential rather than capacity of electrodes; therefore, as long as new chemistries operate reasonably within the electrochemical stability window of carbonate-based electrolytes (as most of the above-mentioned cathode and anode materials do), major changes in the skeleton composition are not mandatory. (2) More effective design and use of electrolyte additives became customary practices, aided by the significant advances in the fundamental knowledge of how “solid electrolyte interphases” (SEI) form on electrode surfaces. These “drop-in” sacrificial components contribute to maintain the electrolyte skeleton compositions more or less statics. (3) Perhaps most importantly, confined by cost consideration, the battery industry has been reluctant to change the existing supply chain, unless there is sufficient incentive or benefit.²⁶

The most generally used organic solvents are mixture of the cyclic carbonate such as ethylene carbonate (EC) or propylene carbonate (PC), and linear carbonate such as dimethyl carbonate (DMC), diethyl carbonate (DEC), and ethyl methyl carbonate (EMC).²⁶ (See Table 1.2.6.)

Table 1.2.6. Representative cyclic and linear carbonates as electrolyte solvents and their characteristics.²⁷

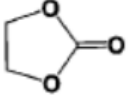
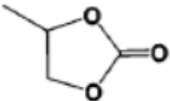
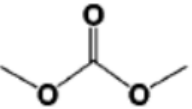
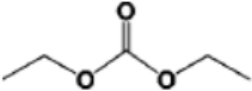
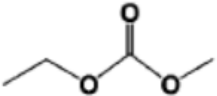
Solvent	Structure	Molecular weight	T _m (°C)	T _b (°C)	T _f (°C)	ε (25 °C)	η/cP (25 °C)
EC		88	36.4	248	160	89.78	1.90 (40 °C)
PC		102	-48.8	242	132	64.92	2.53
DMC		90	4.6	91	18	3.107	0.59
DEC		118	-74.3	126	31	2.805	0.75
EMC		104	-53	110		2.958	0.65

Table 1.2.7. Comparison of lithium salt characteristics²⁸

	LiPF₆	LiBF₄	LiCF₃SO₃	Li(CF₃SO₂)₂N	LiClO₄
Solubility	◎	○	○	◎	◎
Ionic conductivity	◎	○	△	◎	◎
Low-temperature performance	○	△	△	○	○
Thermal stability	X	○	○	○	X
Stability toward Al	○	○	X	X	○
Stability toward Cu	○	○	○	○	○

◎: Excellent, ○: good, △: normal, X: poor.

References

1. C. Liu, Z. G. Neale et al., *Materials Today* Volume 19, 2 March 2016
2. S.R. Bottone, *Galvanic Batteries, Their Theory, Construction and Use, Comprising Primary, Single and Double Fluid Cells. Secondary and Gas Batteries*, NabuPress, 2010
3. Park, J.-K., *Principles and Applications of Lithium Secondary Batteries*. Wiley-VCH Verlag GmbH & Co. KGaA : 2012
4. Tarascon, J.-M.; Armand, M., Issues and challenges facing rechargeable lithium batteries. *Nature* 2001, 414 (6861), 359-367
5. A. Yoshino, in *Lithium-Ion Batteries*, ed. G. Pistoia, Elsevier, 2014, pp. 1–20.
6. L. Croguennec and M. R. Palacin, *J. Am. Chem. Soc.*, 2015, 137, 3140–3156.
7. B. Scrosati, J. Hassoun and Y.-K. Sun, *Energy Environ. Sci.*, 2011, 4, 3287.
8. C. M. Park, J. H. Kim, H. Kim and H. J. Sohn, Li-alloy based anode materials for Li secondary batteries. *Chem. Soc. Rev.* 2010, 39 (8), 3115-3141..
9. W.-J. Zhang, A review of the electrochemical performance of alloy anodes for lithium-ion batteries. *J. Power Sources* 2011, 196 (1), 13-24.
10. J. R. Szczech and S. Jin, Nanostructured silicon for high capacity lithium battery anodes. *Energy Environ. Sci.* 2011, 4 (1), 56-72.
11. B. Scrosati, Recent advances in lithium ion battery materials. *Electrochim. Acta* 2000, 45 (15), 2461-2466
12. Wei Xiao, Jingjing Wang, Hong Wang et al., *J Solid State Electrochem* (2016) 20:2847–2855
13. Gao, Y. and Dahn, J.R. *J. Electrochem. Soc.* 1996, 143, 100-114.
14. Park, J.-K., *Principles and Applications of Lithium Secondary Batteries*. Wiley-VCH Verlag GmbH & Co. KGaA : 2012, 21-87
15. F. Y. Cheng, J. Liang, Z. L. Tao, J. Chen, *Adv. Mater.*, 2011, 23, 15
16. M. Winter, R. J. Brodd, *Chem. Rev.*, 2004, 104 (10), pp 4245–4270
17. Park, J.-K., *Principles and Applications of Lithium Secondary Batteries*. Wiley-VCH Verlag GmbH & Co. KGaA : 2012, 89-139
18. C. M. Park, J. H. Kim, H. Kim and H. J. Sohn, Li-alloy based anode materials for Li secondary batteries. *Chem. Soc. Rev.* 2010, 39 (8), 3115-3141.
19. W.-J. Zhang, A review of the electrochemical performance of alloy anodes for lithium-ion batteries. *J. Power Sources* 2011, 196 (1), 13-24.
20. J. R. Szczech and S. Jin, Nanostructured silicon for high capacity lithium battery anodes. *Energy Environ. Sci.* 2011, 4 (1), 56-72.
21. B. Scrosati, Recent advances in lithium ion battery materials. *Electrochim. Acta* 2000, 45

- (15), 2461-2466.
22. H. Lee, M. Yanilmaz et al., *Energy Environ. Sci.*, 2014,7, 3857 –3886
 23. V. Deimede and C. Elmasides, *Energy Technol.* 2015, 3, 453 – 468
 24. C. M. Costa, M. M. Silva et al., Battery separators based on vinylidene fluoride (VDF) polymers and copolymers for lithium ion battery applications. *RSC Adv.* 2013, 3 (29), 11404.
 25. S. M. Kang et al., Mussel- and Diatom-Inspired Silica Coating on Separators Yields Improved Power and Safety in Li-Ion Batteries. *Chem. Mater.* 2012, 24 (17), 3481-3485
 26. Yamada, Y., Sagane, F., et al., Kinetics of Lithium-Ion Transfer at the Interface between $\text{Li}_{0.35}\text{La}_{0.55}\text{TiO}_3$ and Binary Electrolytes., *The Journal of Physical Chemistry C* 2009, 113, 4528–14532.
 27. Yamada, Y, Sagane, F. et al., Kinetics of Lithium-Ion Transfer at the Interface between $\text{Li}_{0.35}\text{La}_{0.55}\text{TiO}_3$ and Binary Electrolytes. *The Journal of Physical Chemistry C* 2009, 113, 14528–14532.
 28. J.-K., *Principles and Applications of Lithium Secondary Batteries.* Wiley-VCH Verlag GmbH & Co. KGaA : 2012, 146

1.3. Conducting Polymers

1.3.1. Introduction of Conducting Polymers

Compared with other materials like metal and ceramics, conventional polymers like plastics, rubbers, and resins, show low cost, easy to synthesize, high elasticity, but they exhibit low conductivity than insulators or dielectrics. Conducting polymers (CPs), also known as “synthetic metals”, show obvious difference with conventional polymers. The CPs can serve two ends: the advantages of conventional polymers and improved electric conductivity nearby semiconductors to metal’s conductivity. There is a comparison of the conductivities of the CPs with those of conventional conductors shown in Figure 1.3.1.¹

The initial work on the CPs was pioneered by three Nobel laureates, Alan Heeger, Alan MacDiarmid, and Hideki Shirakawa.^{2,3} They discovered an increase of nearly 10 orders of magnitude in the electrical conductivity of polyacetylene (PA) when it was doped with iodine or other acceptors.⁴ Since Heeger et al. discovered the CPs, many researchers are diving into fundamental study and application. As shown in figure 3.0.2., CPs include polyacetylene (PA), polypyrrole (PPy), polyaniline (PANI), poly(3,4-ethylenedioxythiophene) (PEDOT) and poly(p-phenylenevinylene) (PPV) etc.⁵ Their structures are described in Figure 1.3.2. Among them, PANI and PPy are widely used because of their stability and processability despite of their conductivities are relatively low.

However, pure CPs had few limitations such as low sensitivity, poor selectivity, surface poisoning due to adsorbed intermediates, and interference from other species, which is why they have not been commercialized to date.⁶

Thus, recently, CP nanocomposites with enhanced properties have been developed to overcome the inherent limitations of pure CPs.

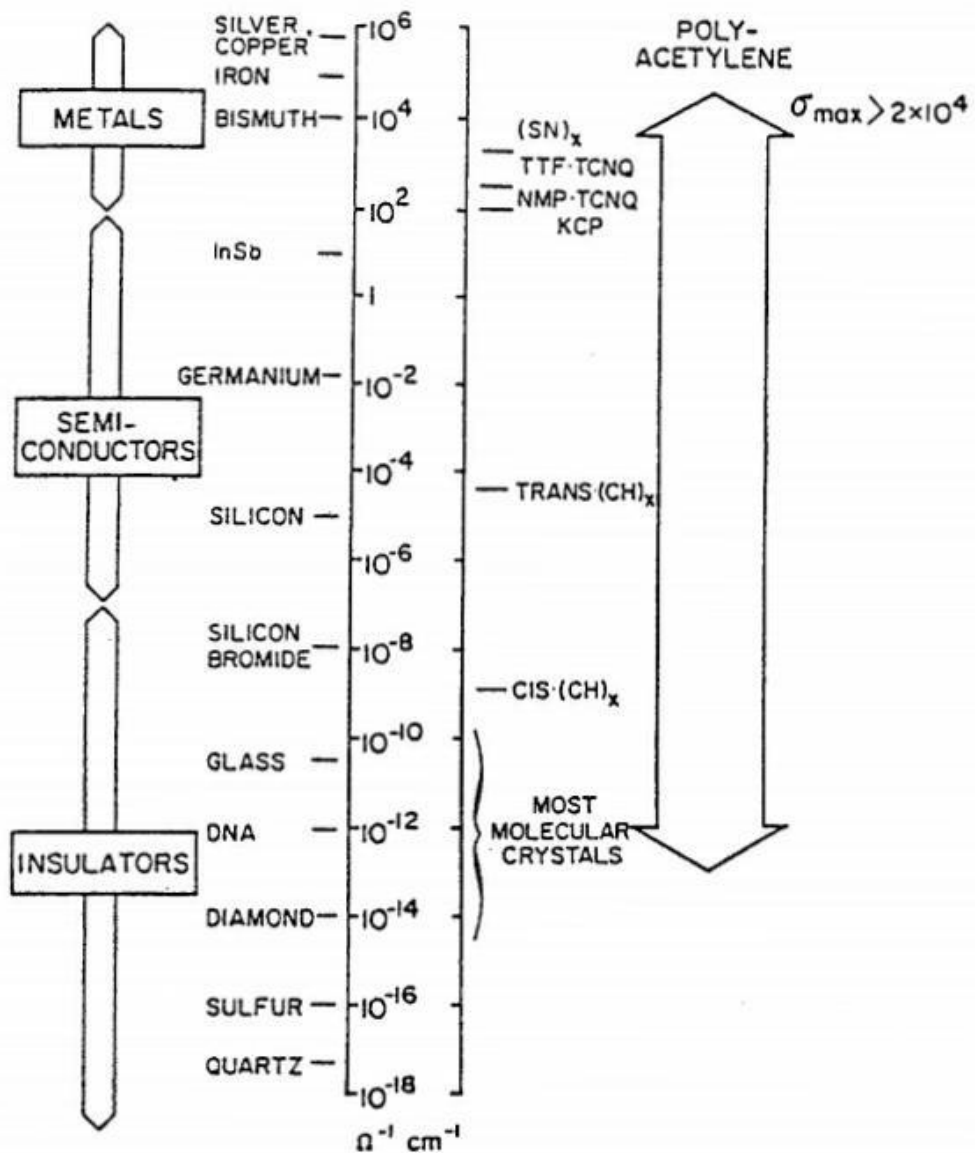


Figure 1.3.1. Comparison of the conductivities of doped conducting polymers with those of conventional conductors.¹

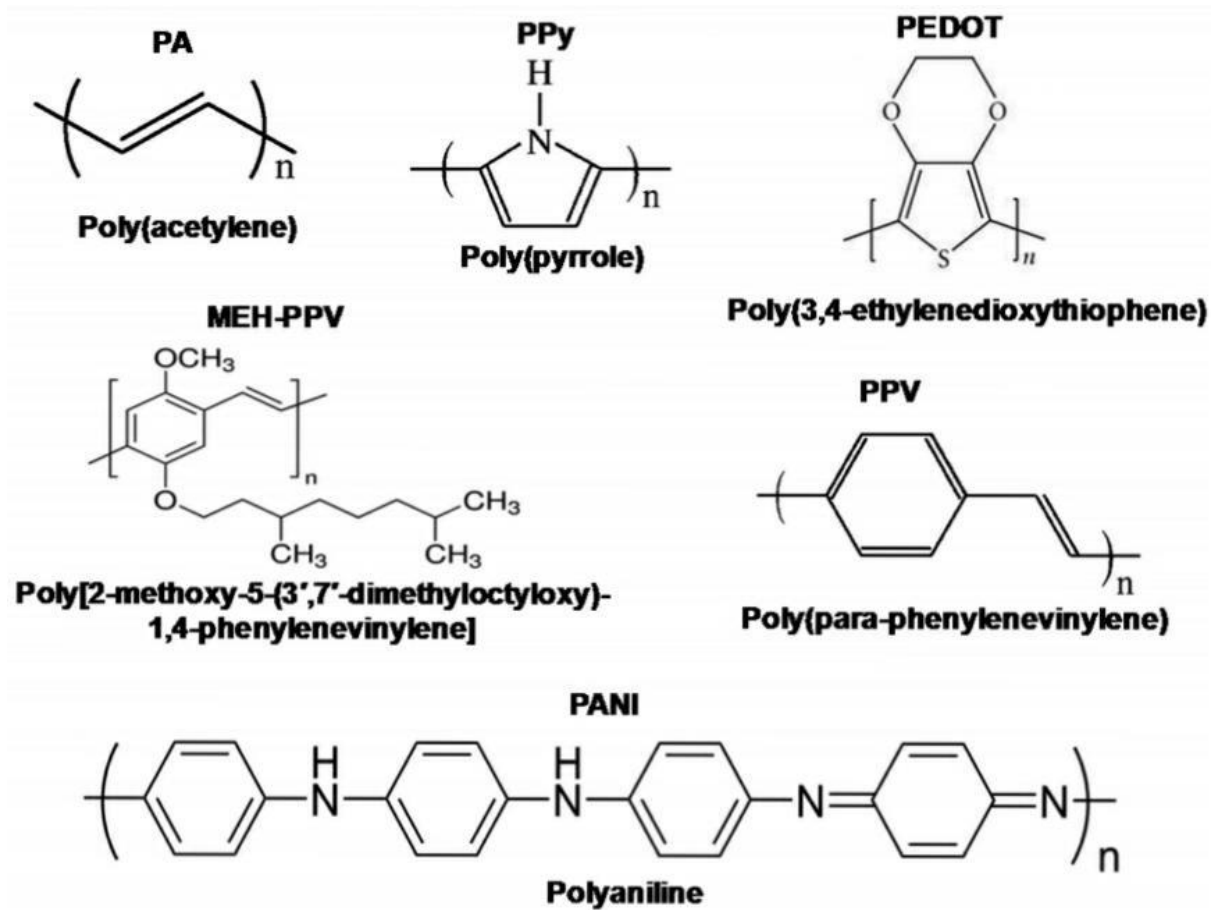


Figure 1.3.2. Molecular structures of some representative conducting polymers⁵

Table 1.3.1. The conductivity, stability and processability of a number of conducting polymers.⁷

Polymer	Conductivity (S/cm)	Stability	Processability
Polyacetylene (PA)	10^3 - 10^5	Poor	Limited
Polyphenylene (PP)	1000	Poor	Limited
Poly(phenylene vinylene) (PPV)	1000	Poor	Limited
Poly(phenylene sulphide) (PPS)	100	Poor	Excellent
Polypyrroles (PPy)	100	Good	Good
Polythiophenes (PT)	100	Good	Excellent
Polyaniline (PANI)	10	Good	Good

1.3.2. Basic Principles of Conducting Polymers

Contrary to the reputations of Shirakawa et al. in 1970's, Letheby et al. was first described in mid-19th century. They investigated the electrochemical and chemical oxidation products of aniline in acidic media. They noted that conducting polymers (CPs) up to the of pH value of media.⁴

CPs are inherently conducting in nature due to the presence of a conjugated π -electron system in their structure. As can be seen in Figure 1.3.3., the conjugated structure with alternating single and double bonds or conjugated segments coupled with atoms providing p-orbitals⁸ for a continuous orbital overlap (e.g. N, S) seems to be necessary for polymers to become intrinsically conducting. This is because just as metals have high conductivity due to the free movement of electrons through their structure, for polymers to be electronically conductive they must possess not only charge carriers but also an orbital system that allows the charge carriers to move in order. For example, polythiophene contains sulfur in aromatic cycle. On the other hand, polyaniline, nitrogen is contained outside.

The conjugated structure can meet the second requirement through a continuous overlapping of S-orbitals along the polymer backbone. Since most organic polymers do not have intrinsic charge carriers, the required charge carriers provided by partial oxidation (p-doping) of the polymer chain with electron acceptors (e.g. I_2 , AsF_5). Polyacetylene is an example of this case. Not only remains partial oxidation of the polymer, there is another case: Partial reduction (n-doping) with electron donors (e.g. Na, K). Through such a doping process, charged defects (e.g. polaron (i.e., radical ions), bipolarons (i.e., dications or dianions) and solitons) are introduced, which could then be available as the charge carriers. (See Figure 3.2.4.)

CPs can be doped with a lot of molecules, such as small salt ions, peptides, or polymers, including polysaccharides and proteins.

In short, "doping" converts insulated polymer into semiconducting bias or conductor to conducting organic polymers. Depending on acceptor dopants, their state of the conductivity can be fluctuated.

Conducting polymers not only exhibit conduction properties, but also exhibit some extraordinary properties such as electronic, magnetic, wetting, optical properties, mechanical, and microwave-absorbing properties.

The properties of hybrid conducting polymers mainly depends on the size, shape, aspect ratio, dispersion, and alignment of the filler (organic-inorganic) within the matrix.

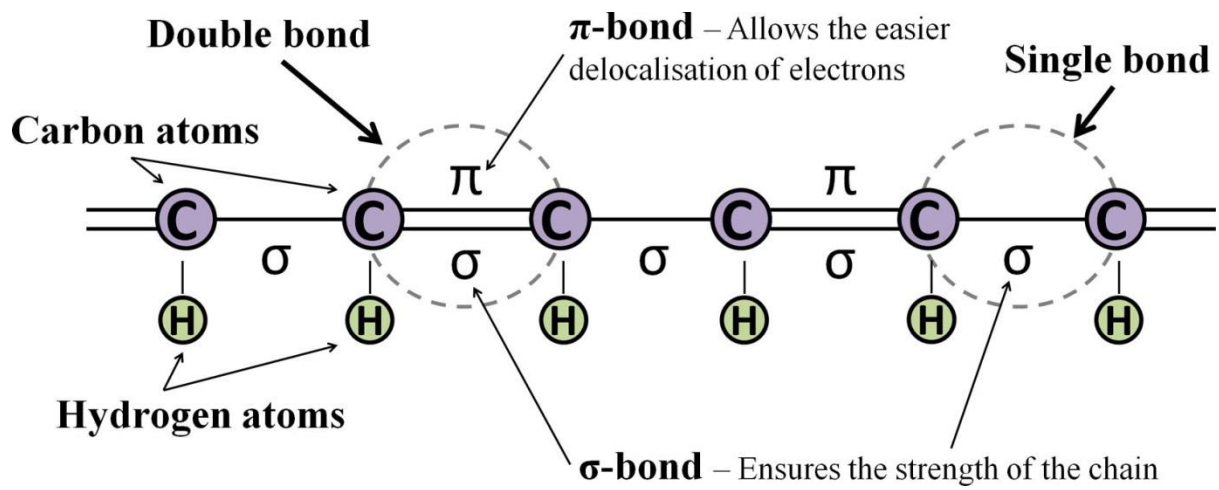


Figure 1.3.3. A simplified schematic of a conjugated backbone: a chain containing alternating single and double bonds.¹⁰

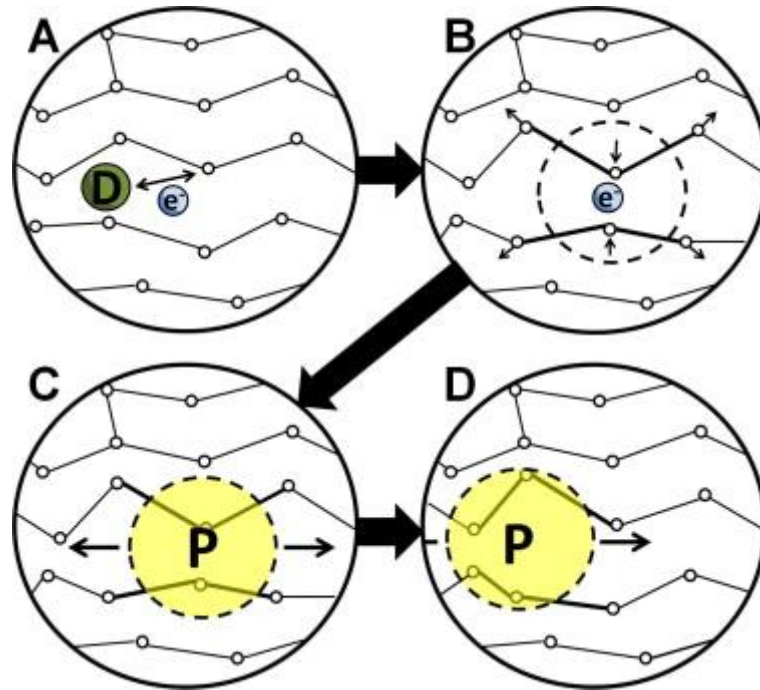


Figure 1.3.4. A simplified explanation of the electrical conductivity of conducting polymers. (A) The dopant removes or adds an electron from/to the polymer chain, creating a delocalized charge. (B) It is energetically favorable to localize this charge and surround it with a local distortion of the crystal lattice. (C) A charge surrounded by a distortion is known as a polaron (a radical ion associated with a lattice distortion). (D) The polaron can travel along the polymer chain, allowing it to conduct electricity.¹⁰

1.3.3. Polymerization mechanism

Conducting polymers (CPs) are normally synthesized via oxidative coupling of monomers. For polymerization, the first step is the oxidation of the monomer, which results in the formation of a radical cation, which then reacts with another monomer or radical cation, forming a dimer. Hence, an obvious classification is the initiation process of polymerization. The three general initiation routes are chemical, electrochemical, and photo-induced oxidation, each having its own advantages and disadvantages. (See Figure 1.3.5.)

First synthesis method, chemical polymerization, requires an oxidizing agent to synthesize the polymer. Monomer/oxidizing agent concentration, temperature, pH parameter, and reaction time can be variables to this method. It involves either step-growth mechanism, or chain-growth mechanism.¹²⁻¹⁷ The main advantage of chemical polymerization is providing diverse available methods to synthesize different CPs and permitting the large-scale production of these materials, which is currently impossible with electrochemical synthesis. Inter alia, chemical polymerization has more options in terms of covalent modification of the CP backbone.¹⁷⁻²²

While chemical polymerization needs an oxidizing agent, the second method, electrochemical polymerization doesn't need an oxidizing agent. However, several monomers are theoretically not able to be electrochemical polymerized and hard to scale up. Electrochemical polymerization of CPs is normally employed by: (1) constant current or galvanostatic; (2) constant potential or potentiostatic; (3) potential scanning/cycling or sweeping methods. High oxidation potential may lead to overoxidation of the polymer also act as cons.^{21,23-27}

The last method, photoinitiation, also known as photopolymerization is the method that overcomes the over oxidation problems. In this process, monomers can be polymerized by exposure to light, or holes. It means, this method need illumination for polymerization. This process can be easily controlled by turning off the light on or off. In photopolymerization, there are two general examples in this method: Direct photopolymerization and photosensitizer-mediated polymerization. In addition, this process provides better control over the shape, size, and physical properties of CPs by tuning the source of the initiator, light intensity, and temperature. However, not all CPs can be synthesized by photoelectrochemical polymerization.²⁸⁻³²

CPs' polymerization not only introduced with aforementioned methods, by extension, also categorized with template-based synthesis procedures to gain various nanostructures. In general, CPs with different nanostructures also can be produced: solid template, molecular template, template-free, electrospinning, and nanoimprinting.

Based on the mechanism and procedure for the fabrication, the methodologies may be classified into three main categories like ex-situ (sequestered) synthesis, in-situ (sequential) synthesis; and one-pot (concurrent) synthesis. (See Figure 1.3.6.)

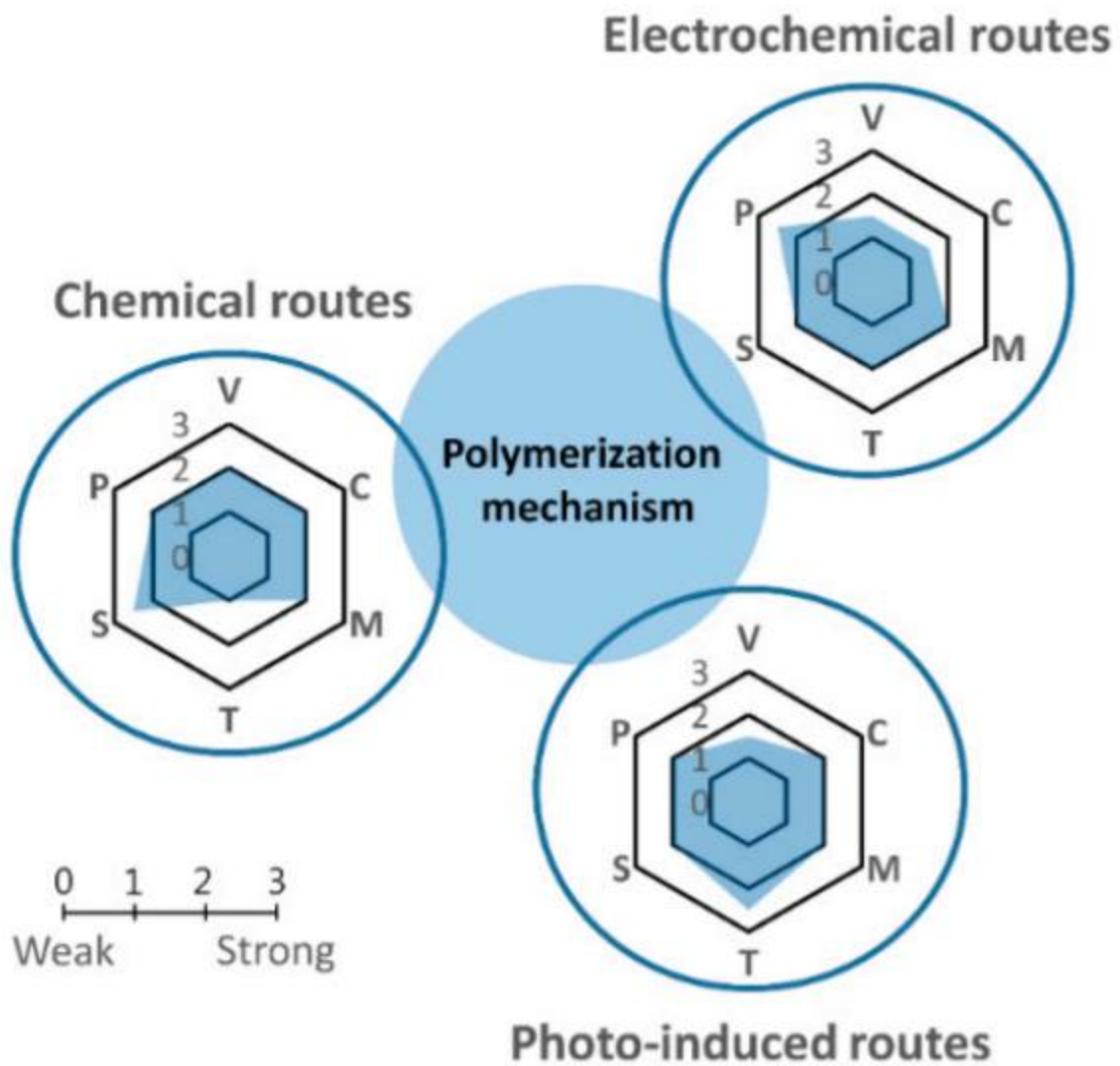


Figure 1.3.5. Schematic comparing the chemical, electrochemical, and photopolymerization mechanisms. V: variables, C: cost effectiveness, M: morphology control, T: time of reaction, and R: resulting purity of the materials.¹¹

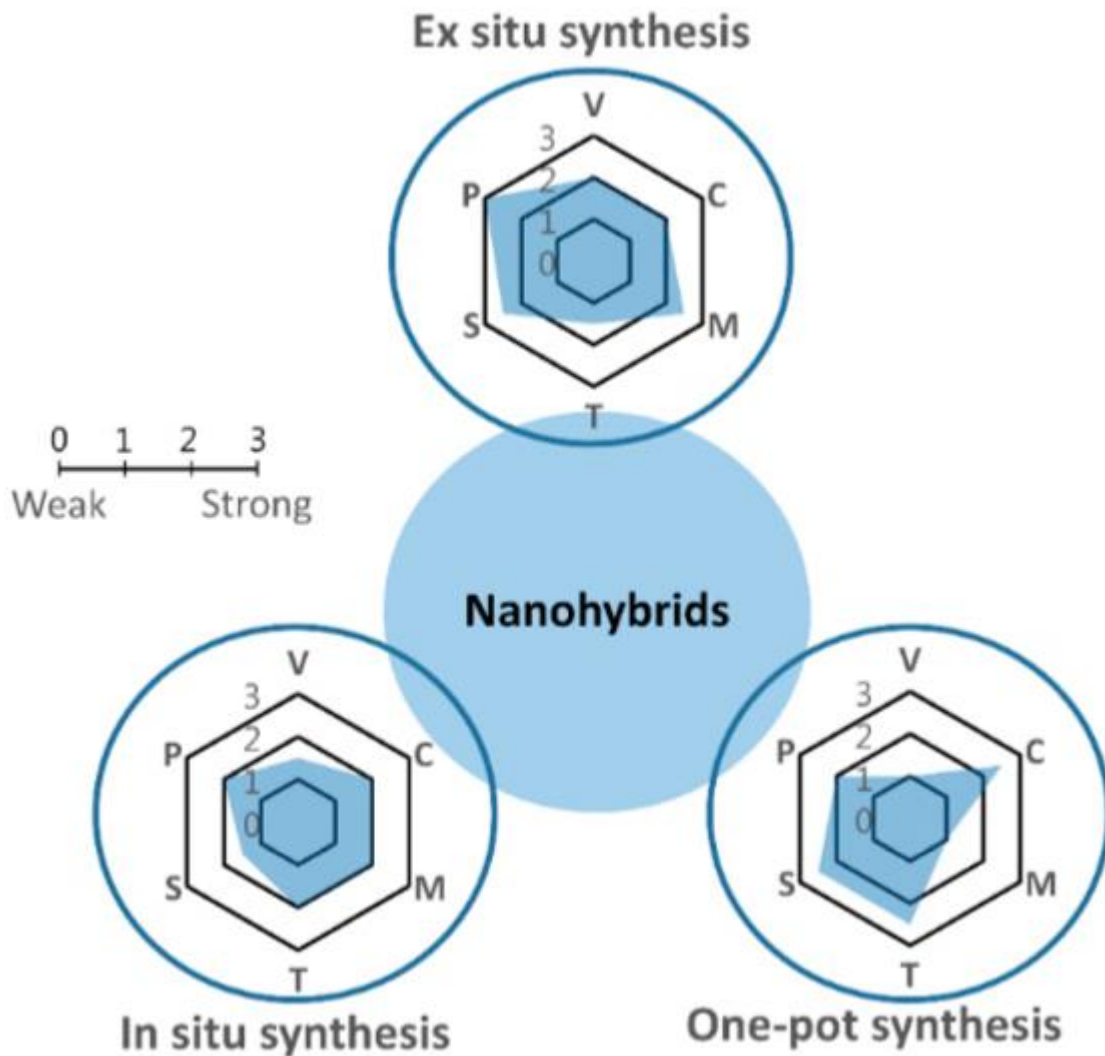


Figure 1.3.6. Schematic of nanohybrid synthesis methods. Each mechanism has been evaluated in terms of variables (V), in which a low value means there are many key variables in the synthesis process; cost (C), in which a low value corresponds to high cost; morphology control (M); time required (T); scalability (S); and purity (P) of products.¹¹

1.3.4. Applications of Conducting Polymers

The increasing number of academic, governmental, and industrial laboratories throughout the world involved in fundamental research and assessment of possible applications of conducting polymers show that this area is interdisciplinary in nature. These materials have allured attention leading to their current use in such fields such as electronic devices, sensors (chemical or biological), catalysis or electro catalysis, energy storage, microwave absorption, EMI shielding and biomedicine. Therefore, the following section discusses the application of CPs in the aforesaid fields separately: solar cells, sensors, transistors and data storage, corrosion inhibitors, lasers used in flat televisions, anti-state substances for photographic film, electromagnetic shielding for computers ‘smart windows’, displays in mobile telephones and mini-format television screens, batteries, electrochromic devices, compact capacitors, anti-static coating and so on.

References

1. T. A. Skotheim et al., Handbook of Conducting Polymers se Second Edition, 27-84
2. Epstein,A. J.& Mele,E. J.(eds) Symposium proceedings 4–5 May 2000.Synth. Met., 125, 1, 38 (2001).
3. Heeger,A. J.Semiconducting and metallic polymers:the fourth generation of polymeric materials (Nobel lecture)., Angew. Chem. Int. Edn40, 2591–2611 (2001).
4. A. J. Heeger, Angew. Chem., Int. Ed., 2001, 40, 2591–2611
5. Srabanti Ghosh, Thandavarayan Maiyalagan et al., Nanoscale, 2016,8, 6921-6947
6. S. Prakash et al., Biosensors and Bioelectronics 41 (2013) 43–53
7. S. Bhadra et al., Progress in Polymer Science 34 (2009) 783–810
8. S. Stafstrom, J. L. Bredas, A. J. Epstein, H. S. Woo, D. B. Tanner, W. S. Huang and A. G. MacDiarmid, Phys. Rev. Lett., 1987, 59, 1464–1467.
9. R. Balint et al., Acta Biomaterialia, 10 (2014) 2341–2353
10. D.N. Nguyen et al., Polymers, 2016, 8, 118
11. Deng, J. et al., Effect of the oxidant/monomer ratio and the washing post- treatment on electrochemical properties of conductive polymers., Ind. Eng. Chem. Res., 2014, 53, 13680–13689.
12. Tantawy, H.R. et al., Chemical effects of a solvent-limited approach to HCl-doped polyaniline nanopowder synthesis., J. Phys. Chem. C, 2013, 118, 1294–1305.
13. Mu, J.; Ma, G.; Peng, H.; Li, J.; Sun, K.; Lei, Z. Facile fabrication of self-assembled polyaniline nanotubes doped with d-tartaric acid for high-performance supercapacitors., J. Power Sources, 2013, 242, 797–802.
14. Lu, Q.; Zhao, Q.; Zhang, H.; Li, J.; Wang, X.; Wang, F. Water dispersed conducting polyaniline nanofibers for high-capacity rechargeable lithium—oxygen battery. ACS Macro Lett., 2013, 2, 92–95.
15. Lu, S.; Zhang, X.; Feng, T.; Han, R.; Liu, D.; He, T. Preparation of polypyrrole thin film counter electrode with pre-stored iodine and resultant influence on its performance., J. Power Sources 2015, 274, 1076–1084.
16. Severt, S.Y.; Ostrovsky-Snider, N.A.; Leger, J.M.; Murphy, A.R. Versatile method for producing 2D and 3D conductive biomaterial composites using sequential chemical and electrochemical polymerization., ACS Appl. Mater. Interfaces 2015, 7, 25281–25288.
17. Deng, J.; Wang, X.et al., Effect of the oxidant/monomer ratio and the washing post-treatment on electrochemical properties of conductive polymers. Ind. Eng. Chem. Res. 2014, 53, 13680–13689.

18. Tantawy, H.R.; Weakley, A.T. et al., Chemical effects of a solvent-limited approach to HCl-doped polyaniline nanopowder synthesis. *J. Phys. Chem. C* 2013, 118, 1294–1305.
19. Mu, J.; Ma, G.; Peng, H.; Li, J.; Sun, K.; Lei, Z., Facile fabrication of self-assembled polyaniline nanotubes doped with d-tartaric acid for high-performance supercapacitors., *J. Power Sources* 2013, 242, 797–802.
20. Lu, Q.; Zhao, Q. et al., Water dispersed conducting polyaniline nanofibers for high-capacity rechargeable lithium—oxygen battery. *ACS Macro Lett.* 2013, 2, 92–95.
21. Lu, S.; Zhang, X. et al., Preparation of polypyrrole thin film counter electrode with pre-stored iodine and resultant influence on its performance., *J. Power Sources* 2015, 274, 1076–1084.
22. Severt, S.Y.; Ostrovsky-Snider, N.A. et al., Versatile method for producing 2D and 3D conductive biomaterial composites using sequential chemical and electrochemical polymerization., *ACS Appl. Mater. Interfaces* 2015, 7, 25281–25288.
23. Lee, S.B.; Lee, S.M. et al., Preparation and characterization of conducting polymer nanocomposite with partially reduced graphene oxide., *Synth. Met.* 2015, 201, 61–66.
24. Feng, W.; Wan, A.S. et al., Interfacial bonding and morphological control of electropolymerized polythiophene films on ZnO., *J. Phys. Chem. C* 2013, 117, 9852–9863.
25. Zhang, X.; Wang, S.; et al., Influence of doping anions on structure and properties of electro-polymerized polypyrrole counter electrodes for use in dye-sensitized solar cells., *J. Power Sources* 2014, 246, 491–498.
26. Chen, S.; Zhitomirsky, I. et al., Polypyrrole electrodes doped with sulfanilic acid azochromotrop for electrochemical supercapacitors., *J. Power Sources* 2013, 243, 865–871.
27. McGarry, S.P.; Barrera Ramirez, E.A. et al., Modelling electrochemical control of percolation conductivity in short-chain templated conducting polymers., *Synth. Met.* 2015, 200, 156–163.
28. Sangermano, M.; Sordo, F. et al, One-pot photoinduced synthesis of conductive polythiophene-epoxy network films., *Polymer* 2013, 54, 2077–2080.
29. Yamada, K.; Yamada, Y. et al., Three-dimensional photochemical microfabrication of poly(3,4-ethylenedioxythiophene) in transparent polymer sheet., *Thin Solid Films* 2014, 554, 102–105.
30. Janáky, C.; Chanmanee, W. et al, Mechanistic aspects of photoelectrochemical polymerization of polypyrrole on a TiO₂ nanotube array., *Electrochim. Acta* 2014, 122, 303–309.
31. Ngaboyamahina, E.; Cachet, H. et al., Photo-assisted electrodeposition of an electrochemically active polypyrrole layer on anatase type titanium dioxide nanotube arrays.,

- Electrochim. Acta 2014, 129, 211–221.
32. Su, P.G.; Peng, Y.T., Fabrication of a room-temperature H₂S gas sensor based on PPy/WO₃ nanocomposite films by in-situ photopolymerization., *Sens. Actuators B Chem.* 2014, 193, 637–643.
33. M.H. Naveen et al., *Applied Materials Today*, 9 (2017) 419–433

Chapter 2. Study on Si-conducting polymer core-shell anodes for lithium-ion batteries

2.1. Introduction

Silicon(Si) anode is one of the promising anode materials to replace graphite due to following reasons: (1) Si possesses the highest gravimetric capacity (4200 mA h/g, lithiated to $\text{Li}_{4.4}\text{Si}$)¹ and volumetric capacity (9786 mA h/cm³, calculated based on the initial volume of Si) other than lithium metal; (2) Si exhibits an appropriate discharge voltage at c.a. 0.4 V in average, which finds a good balance between retaining reasonable open circuit voltage and avoiding adverse lithium plating process^{2,3} (3) Si is abundance in the earth crust, potentially inexpensive, eco-friendly, and non-toxic.⁴ However, drastic volume expansion (around 360% for $\text{Li}_{4.4}\text{Si}$) and huge stress generation are accompanied with the lithiation/delithiation process of Si, the formation of unstable thick solid-electrolyte-interface (SEI) layers and depletion of electrolyte, which will make critical capacity fading. Furthermore, Si has low electrical conductivity and sluggish lithium-ion diffusivity. These fatal flaws hinder the commercialization of Si anode.⁵⁻⁸

To overcome the disadvantages of the Si anode, there are significant attempts to solve these problems. The strategies investigated include Si material design through nanostructures,⁹⁻¹³ porous structures,¹⁴⁻¹⁷ or nanocomposites¹⁸⁻²⁰. Si electrode design with combined nanoparticles and microparticles²¹ or with 3D microchannels,²² addition of electrolyte additives,²³ and the use of novel binders.^{24, 25}

In the case of Si composite materials, conducting polymers are also used to make improvements. Conducting polymers are polymeric materials that display high conductivities, good electrochemical activity, unique optical properties, and biocompatibility. Because of these interesting properties, CPs have received special attention as promising candidates in many areas of nanoscience and nanotechnology. However, pure CPs had few limitations such as low sensitivity, poor selectivity, surface poisoning due to adsorbed intermediates, and interference from other species, which is why they have not been commercialized to date.²⁶ Thus, recently, CP nanocomposites with enhanced properties have been developed to overcome the inherent limitations of pure CPs.

Herein, we studied simple methods to synthesize conducting polymer coated Si anode to modify the limitations of Si anode. First synthesis is fabricating PPy coated Si anode by vapor phase polymerization. Another one is synthesizing SO_3 doped PANI coated Si anode. We used two-dimensional (2D) silicon sheet, which was synthesized by magnesiothermic reduction reaction. In the case of Si@PPy, initial coulombic efficiency (ICE) was 85%, because, overoxidation occurs during synthesis. On the other hand, in the case of SO_3 doped polyaniline (PANI), it shows 98.4%, 13.4% higher than PPy coated Si. 2D Si flake @ PPy and 2D Si flake @ SO_3 doped PANI were synthesized

to improve the disadvantages of Si anode. 2D Si flake @ PPy adopted vapor phase polymerization to simplify the coating method, but, it was hard to gain uniformly coated sample, and overoxidation reaction occurs through the reaction. Spring from overoxidation reaction, it increased Li^+ intercalation but deintercalation didn't keep up with the amount of intercalated Li^+ . Overoxidation led the drop of the initial coulombic efficiency. On the other hand, 2D Si flake @ SO_3 doped PANI displayed uniformly coated Si anode and prevented overoxidation through dissolving and reconstruction in NMP solution. Moreover, 2D Si flake @ SO_3 doped PANI exhibited high initial coulombic efficiency, good cycling performance, and suppressed expansion.

2.2. Experimental Section

2.2.1. **Synthesis of 2D Silicon flake (Si flake):** The 2D Si flake was synthesized by magnesiothermic reduction reaction and subsequent simple acid leaching process. Mix 1g of talc powder and 0.7 g of magnesium powder. The mixture was transferred to an alumina boat in argon (Ar) atmosphere. This alumina boat was placed in a center of tube furnace and heated to 700 °C for 3hrs. After then, reacted powder was dissolved in 100 mL of deionized water under 300 rpm for 3hrs. Subsequently, 1 M HCl was added to this dissolved solution, and stirred for 3hrs at room temperature. Remained by-product, MgO was eliminated in this process. Rinsed with ethanol and deionized water for several times.

2.2.2. **Synthesis of 2D Si flake @ Polypyrrole (PPy):** To synthesize PPy, vapor phase polymerization method was used in this process. First, mix as-synthesized 2D Si flake and $\text{Fe}(\text{NO}_3)_3 \cdot 9\text{H}_2\text{O}$. (1:2 wt%) Place this mixture flatways into the entrance of the three-neck round flask. Simultaneously, pyrrole monomer and ethanol into the center of three-neck round flask. Sealing the entrance of the three-neck flask and heated to 70 °C for 15 min. After reaction, rinsed with ethanol and deionized water for several times to remove remained unreacted $\text{Fe}(\text{NO}_3)_3 \cdot 9\text{H}_2\text{O}$.

2.2.3. Synthesis of 2D Si flake @SO₃ doped polyaniline

Preparation of hydrochloric polyaniline salt: Before coated with SO₃ doped polyaniline, hydrochloric polyaniline salt was synthesized. Disperse 40mM of aniline monomer in 1M HCl 40mL. (Denoted as solution A) Disperse 14mM of APS in 1M HCl 20mL. (Denoted as solution B.) After then, put solution B into solution A and stirring for 2hrs at room temperature. During reaction, the color of the solution turns into black. After the reacted solution. After filtration, rinsed with 0.01M of HCl aqueous solution, ethanol, and acetone in order, to remove left unreacted by-product. After filtration, dry at 80 °C in oven. The color of the powder is dark green.

Synthesis of polyaniline salt: After drying, as-synthesized product need to leach with NaOH before synthesizing SO₃ doped PANI. Sonicate as-fabricated hydrochloric polyaniline salt fully dissolved in NMP. After sonication, input 1M NaOH to delaminate Cl⁻. Leach 1M NaOH for 2days. After vigorous stirring, rinsed with deionized water for several times to eliminate remained by-product (in this case, sodium chloride (NaCl)) and dry at 80 °C.

Synthesis of 2D Si flake @ SO₃ doped PANI: Mix uniformly polyaniline salt and camphorsulfonic acid (CSA) in a weight ratio of 1:4. Stirring this powder in NMP and stirring until fully dissolved. Input 2D Si flake in this solution during stirring. Stirring for 4 hours. After reaction, dilute NMP with acetone and rinse several times to remove residual NMP.

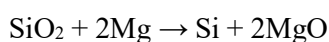
Before grafting concept on 2D Si flake, commercial Si nanoparticle (NP) was used.

2.2.4. Characterization: To characterize these synthesized samples, several tools were used. Scanning electron microscopy (SEM, S-4800, Hitachi) at an accelerating voltage of 10 kV was used to characterize morphologies of 2D Si flake and 2D Si flake @ conducting polymer samples. The dimensions and internal structures of 2D Si flake and 2D Si flake @ conducting polymer were determined using TEM (JEOL-2100) at an acceleration voltage 200 kV. To investigate the microstructures of samples, X-ray diffraction (XRD) analyses (D8 ADVANCE, Bruker) were performed using Cu-K α radiation ($\lambda = 1.5418 \text{ \AA}$) between 10 and 90°. To quantify the elements, Energy-dispersive X-ray spectroscopy (EDS) was used to measure.

2.2.5. Electrochemical measurements: For the electrochemical measurements of Si, the anode was prepared by mixing 80 wt% active material (Si, carbon coated Si (denoted as Si@C) Si @ PPy), 10 wt% of super P and 10 wt% of binder (6 wt% of CMC / 35% poly(acrylic acid) (PAA) (Aldrich) in deionized water with a mixer (Thinky mixer, ARE310) at 2200 rpm for 15 min. Another active materials, Si@SO₃ doped PANI, super P, binder (6 wt% of CMC / 35% PAA (Aldrich) in deionized water at a weight ratio of 70:15:15. The coin-type half-cell (2016R) was assembled in an Ar-filled glove box with oxygen and water less than 1 ppm. The Li metal foil was used as counter electrode and micro porous polyethylene film (Celgard 2400) was used as a separator. The electrolyte consisted of a solution of 1.3M LiPF₆ in a mixture of ethylene carbonate (EC)/diethyl carbonate (DEC) (3:7, v/v) with 10% fluorinated ethylene carbonate (FEC) additive in all half-cell. Each sample was compared with 2D silicon flake and carbon coated 2D silicon flake.

2.3. Results and Discussion

2D Si flake was synthesized by magnesiothermic reduction reaction. Magnesiothermic reduction was first suggested by Bao et al. as one of replacements of conventional carbothermic reduction reaction. During magnesiothermic reduction reaction, magnesium melted at 650°C and reduced silica (SiO₂) into silicon simultaneously.²⁷ It makes possible to reduce SiO₂ in lower temperature. Following equation explains the magnesiothermic reduction reaction between silica and magnesium.



Idea of raw material is derived from Ryu et al.'s paper.²⁸ Talc is one of the clay materials, which structure is composed of Si₂O₅ sheets with magnesium sandwiched between sheets in octahedral sites. Because of its structure, it is possible to gain 2D silicon flake through reaction. After reaction, hydrochloric acid (HCl) used as an etchant to remove byproducts like magnesia (MgO). Before applying conducting polymer coating system, as-synthesized 2D Si flake was confirmed. A scanning electron microscopy (SEM) image of 2D Si flake shows that **Figure 2.3.3. a)** shows the X-ray diffraction (XRD) patterns of the as-synthesized 2D Si flake. 2D Si flake accorded with XRD patterns of Si. Magnesium silicide or magnesium silicate, which are the byproducts of synthesis, they were not detected. It approves that 2D Si flake contains fully silicon structures without byproducts through magnesiothermic reduction reaction and HCl leaching process. To characterize the exact amount of Si and O, energy-dispersive X-ray spectroscopy (EDS) was employed. **(Figure 2.3.2. a)** According to the EDS data, 2D Si flake powders contain 89.87 wt% of Si and 11.13 wt% of O.

Aforementioned in introduction, we suggested two methods to synthesize the core-shell structured conducting polymers coated on Si. In case of 2D Si flake @ PPy, it shows that the particle diameters are few micrometer-sized porous flake materials covered with some sub-micron sized particles. Several particles blocked the pore of flakes. **(Figure 2.3.1. b)** On the other hand, in the case of 2D Si flake @ SO₃ doped PANI, it shows that the particles coated more flimsy particles than 2D Si flake @ PPy. While 2D Si flake @ PPy contain 44.93 wt% of C, 9.47 wt% of N, 12.09 wt% of O, and 34.31 wt% of Si, 2D Si flake @ SO₃ doped PANI contain 9.62 wt% of C, 5.38 wt% of O, and 85.00 wt% of Si. **(Figure 2.3.4. d)** Assuming contents of the conducting polymers approximately, 2D Si flake @ PPy contains 54.4 wt% and 2D Si flake @ SO₃ doped PANI contains 15.00 wt%.

However, both 2D Si flake @ PPy and 2D Si flake @ SO₃ doped PANI, there are no peaks matched with conducting polymers, because, conducting polymers have relatively low contents than silicon and they have amorphous structure. **(Figure 2.3.3. b)**

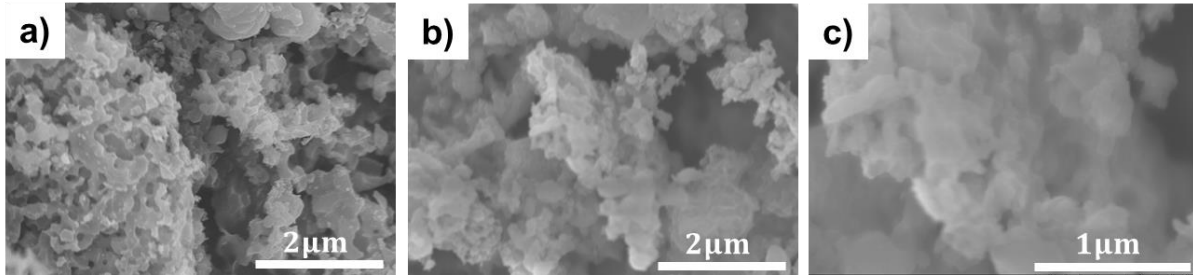


Figure 2.3.1. SEM images of 2D Si flake (a) and 2D Si flake@PPy. (b) to c)).

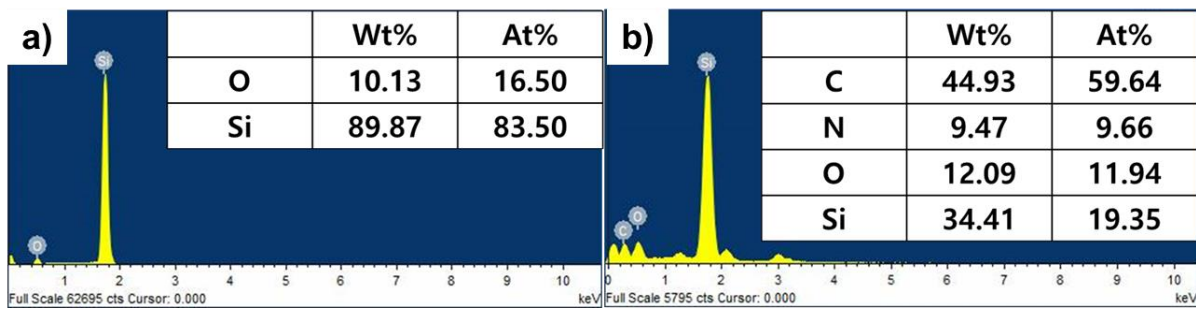


Figure 2.3.2. EDS data of a) 2D Si flake and b) 2D Si flake@PPy

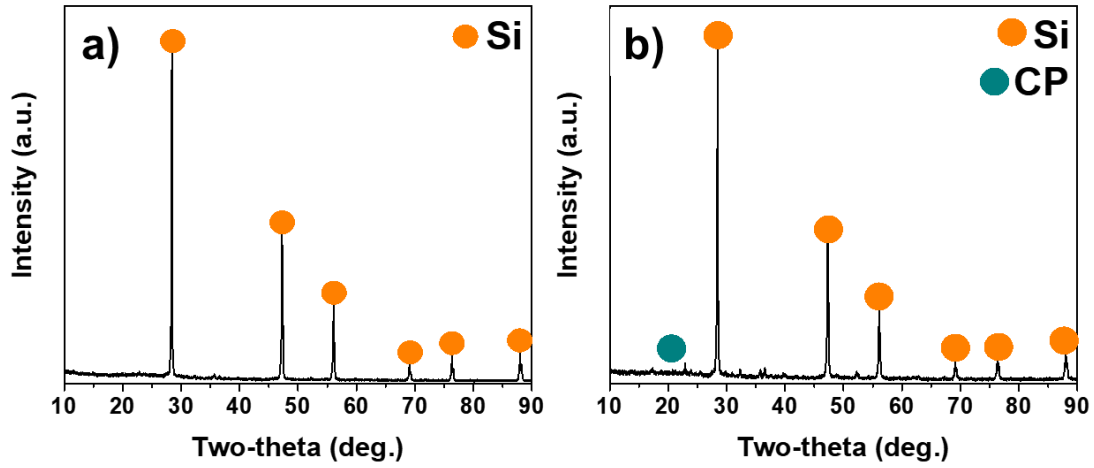


Figure 2.3.3. XRD patterns of a) 2D Si flake and b) 2D Si flake@conducting polymers.

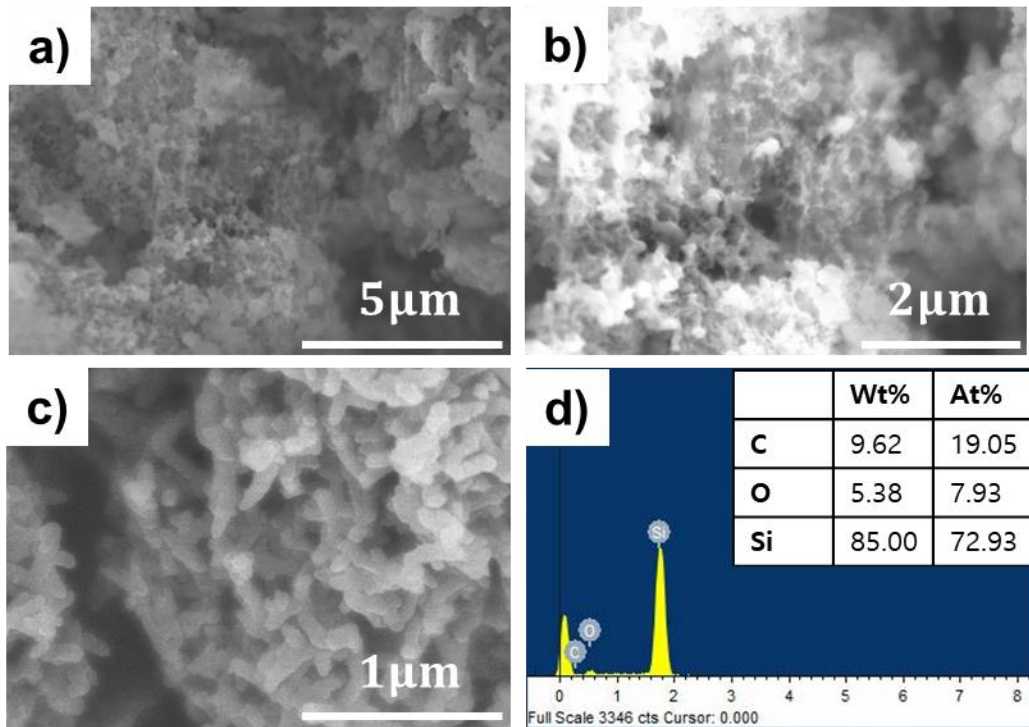


Figure 2.3.4. SEM images of 2D Si flake@SO₃ doped PANI in an a) low magnitude, and b) high magnitude. c) is a high magnitude of PANI hydrochloric salt, and d) is an EDS data of the 2D Si flake@SO₃ doped PANI.

To confirm structures of materials, transmission electron microscopy (TEM) was used. In the case of 2D Si flake @ PPy, although its contents were more than 50 wt% in EDS data, there was partially coated in Si. Several section of sample was not coated or more than 20nm thickness of conducting polymers were coated on sample. Thickness distribution of the sample was too big to show that uniformly coated core-shell structure whereas 2D Si flake @ SO₃ doped PANI was 10-20nm coated on sample. (**Figure 2.3.5.**)

Through these data, we can say that 2D Si flake @ SO₃ doped PANI was more uniformly coated than 2D Si flake @ PPy, because of coating method. Synthesizing 2D Si flake @ PPy is much easier than synthesizing 2D Si flake @ SO₃ doped PANI. However, homogeneity of coating easily influenced on mixing state and condition of sampling owing to vapor phase polymerization (VPP).

Electrochemical performances of 2D Si flake @ PPy and 2D Si flake @ SO₃ doped PANI electrodes were tested in the potential range 0.005-1.5V (versus Li/Li⁺) in a coin-type half cell (2016R). To compare with these electrodes, 2D Si flake (denoted as bare 2D Si flake in **Figure 2.3.6.**) and carbon coated 2D Si flake electrodes were tested in same condition.

Both conducting polymer coated samples initial coulombic efficiency drop occurred resulted in their percentage of silicon is lower than bare 2D Si flake. In the case of Si@PPy, initial coulombic efficiency (ICE) was 85%, because, overoxidation occurs during synthesis. Resulted from overoxidation, deintercalation of Li ions are less than intercalated one, therefore it led the capacity drop. On the other hand, in the case of SO₃ doped polyaniline (PANI), it shows 98.4%, 13.4% higher than PPy coated Si. Through dissolving and coating in NMP solution, it prevents overoxidation, so as to hinder the capacity drop.

Although ICE is smaller than as-synthesized 2D Si flake, their cycle performance is nearby 85% (See **Figure 2.3.6. c**) to 98.4% (**Figure 2.3.6. d**). After 50 cycles up

Volume expansion of Si-based electrodes during repeated cycles is one of the critical points. The thickness of bare 2D Si flake electrodes was 11 μm before cycle. After 50 cycle, the thickness of bare 2D Si flake electrode was 32 μm. It means that the volume expansion of bare 2D Si flake is about 190% during cycling process. On the other hand, initial thickness of 2D Si flake @ SO₃ doped PANI electrode was 20 μm, and after 50 cycles, it was 37 μm. It only expanded about 85% up comes from the effect of the coating layers.

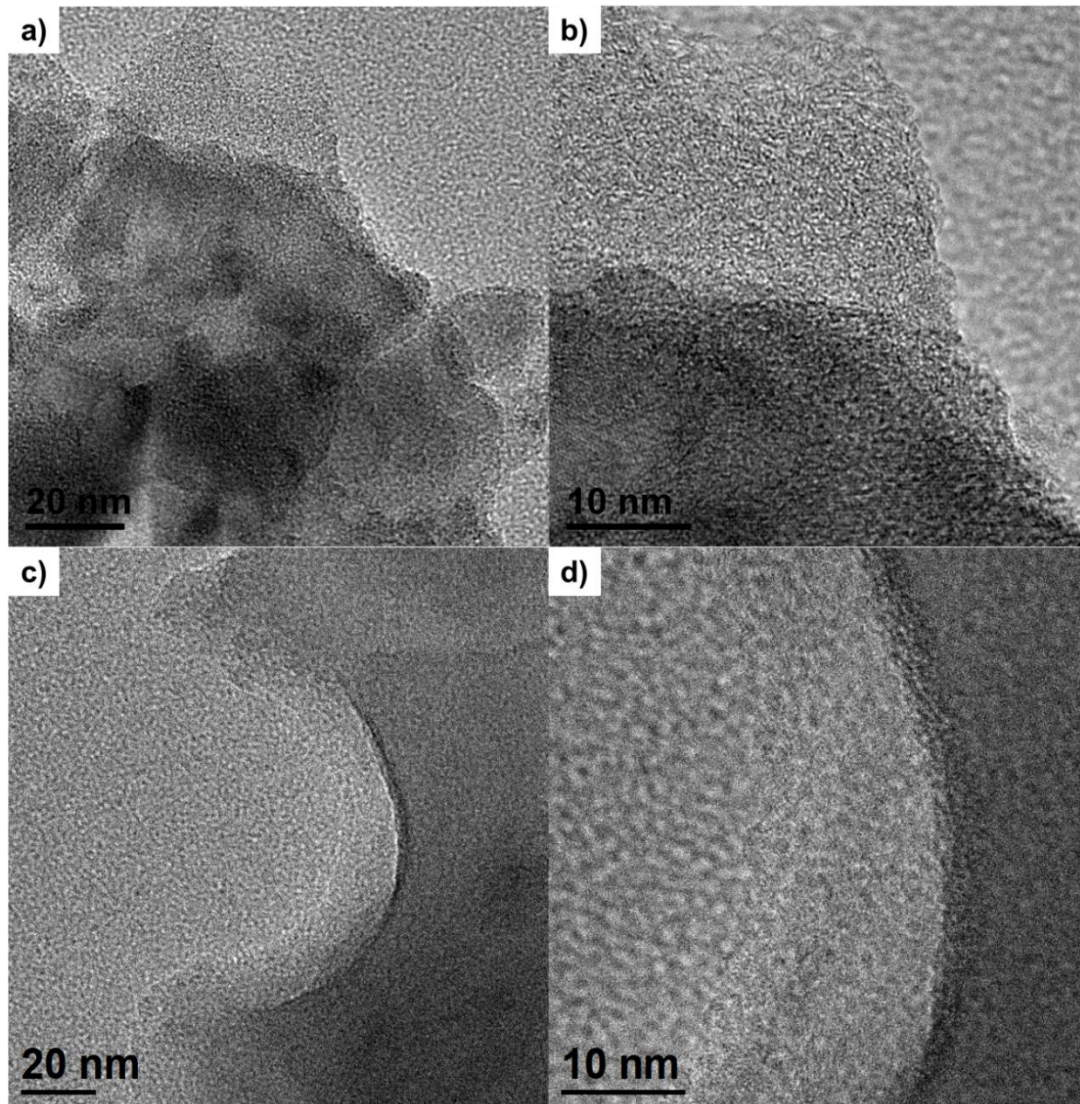


Figure 2.3.5. TEM images of 2D Si flake@PPy (a) to b)) and 2D Si flake@SO₃ doped PANI (c) to d)

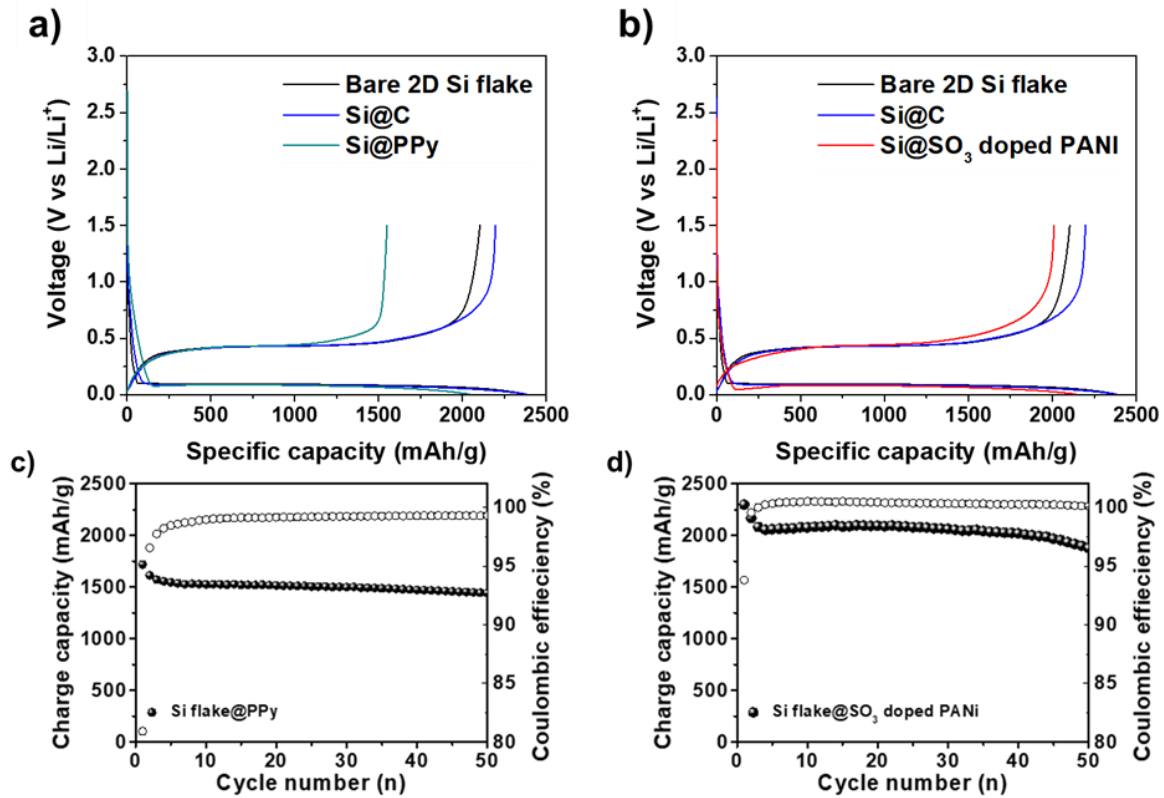


Figure 2.3.6. Electrochemical performance of Si@PPy and Si@SO₃-doped PANI electrodes. A) and b) are first cycle of each material. First cycle voltage profiles obtained at the 0.1C between 0.005V to 1.5V. Cycle performance of Si@PPy and Si@SO₃-doped PANI at rate of 0.5C.

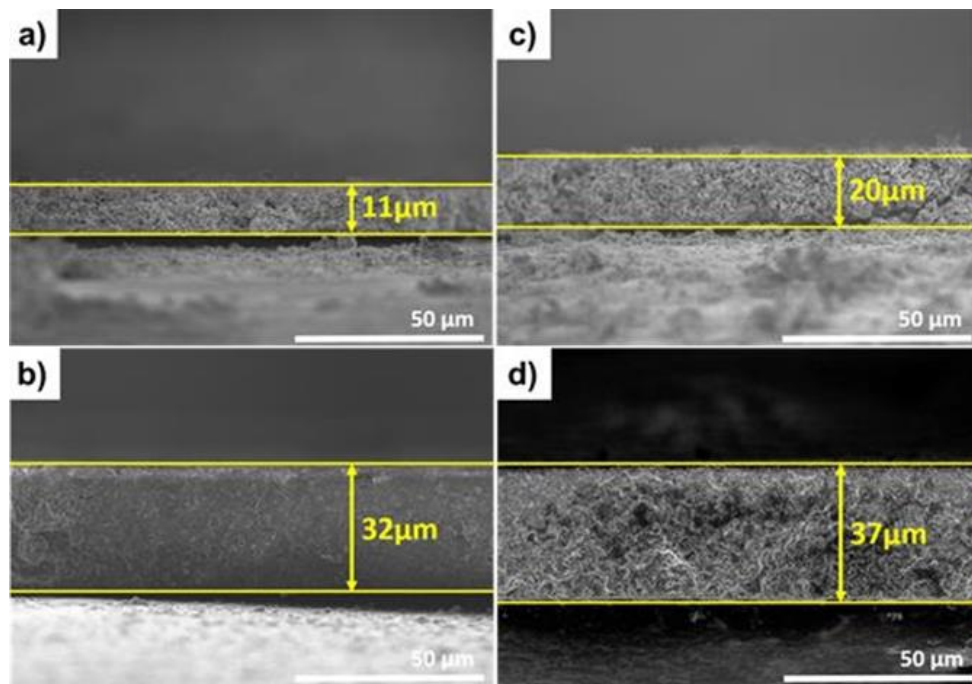


Figure 2.3.7. Cross-sectional SEM images of electrode before and after cycle. a) as-synthesized 2D Si flake electrode before cycle and b) is after 50 cycles of 2D Si flake electrode. c) is 2D Si flake @ SO₃ doped PANI electrode before cycle and d) is after 50 cycles of 2D Si flake @ SO₃ doped PANI electrode.

2.4. Conclusion

In summary, 2D Si flake @ PPy and 2D Si flake @ SO₃ doped PANI were synthesized to improve the disadvantages of Si anode. 2D Si flake @ PPy adopted vapor phase polymerization to simplify the coating method, but, it was hard to gain uniformly coated sample, and overoxidation reaction occurs through the reaction. Spring from overoxidation reaction, it increased Li⁺ intercalation but deintercalation didn't keep up with the amount of intercalated Li⁺. Overoxidation led the drop of the initial coulombic efficiency. On the other hand, 2D Si flake @ SO₃ doped PANI displayed uniformly coated Si anode and prevented overoxidation through dissolving and reconstruction in NMP solution. Moreover, 2D Si flake @ SO₃ doped PANI exhibited high initial coulombic efficiency, good cycling performance, and suppressed expansion. Through coated with conducting polymers, this will open up one potential to Si anode materials to commercialize and utilize in industrial sites.

References

1. B.A. Boukamp, G.C. Lesh, R.A. Huggins, *J. Electrochem. Soc.* 128 (1981) 725–729.
2. W.J. Zhang, *J. Power Sources* 196 (2011) 13–24.
3. B. Liang, Y. Liu, Y. Xu, *J. Power Sources* 267 (2014) 469–490.
4. H. Wu, Y. Cui, *Nano Today* 7 (2012) 414–429.
5. W.J. Zhang, *J. Power Sources* 196 (2011) 13–24.
6. J.H. Ryu, J.W. Kim, Y.-E. Sung, S.M. Oh, *Electrochem. Solid-State Lett.* 7 (2004) A306–A309.
7. M.A. Rahman, G. Song, A.I. Bhatt, Y.C. Wong, C. Wen, *Adv. Funct. Mater.* 26 (2016) 647–678.
8. L.Y. Beaulieu, K.W. Eberman, R.L. Turner, L.J. Krause, J.R. Dahn, *Electrochem. Solid-State Lett.* 4 (2001) A137–A140.
9. H. Kim, M. Seo, M.-H. Park and J. Cho, *Angew. Chem., Int. Ed.*, 2010, 49, 2146–2149.
10. N. Liu, H. Wu, M. T. McDowell, Y. Yao, C. Wang and Y. Cui, *Nano Lett.*, 2012, 12, 3315–3321.
11. L. Y. Yang, H. Z. Li, J. Liu, Z. Q. Sun, S. S. Tang and M. Lei, *Sci. Rep.*, 2015, 5, 10908.
12. J. Graetz, C. Ahn, R. Yazami and B. Fultz, *Electrochem. Solid-State Lett.*, 2003, 6, A194–A197.
13. N. Liu, Z. Lu, J. Zhao, M. T. McDowell, H.-W. Lee, W. Zhao and Y. Cui, *Nat. Nanotechnol.*, 2014, 9, 187–192.
14. R. Yi, F. Dai, M. L. Gordin, S. Chen and D. Wang, *Adv. Energy Mater.*, 2013, 3, 295–300.
15. N. Liu, K. Huo, M. T. McDowell, J. Zhao and Y. Cui, *Sci. Rep.*, 2013, 3, 1919.
16. J. Song, S. Chen, M. Zhou, T. Xu, D. Lv, M. L. Gordin, T. Long, M. Melnyk and D. Wang, *J. Mater. Chem. A*, 2014, 2, 1257–1262.
17. G. Hwang, H. Park, T. Bok, S. Choi, S. Lee, I. Hwang, N.-S. Choi, K. Seo and S. Park, *Chem. Commun.*, 2015, 51, 4429–4432.
18. M. Li, J. Gu, X. Feng, H. He and C. Zeng, *Electrochim. Acta*, 2015, 164, 163–170.
19. D.-H. Lee, H.-W. Shim and D.-W. Kim, *Electrochim. Acta*, 2014, 146, 60–67.
20. H. K. Han, C. Loka, Y. M. Yang, J. H. Kim, S. W. Moon, J. S. Cho and K.-S. Lee, *J. Power Sources*, 2015, 281, 293–300.
21. M. Wu, J. E. C. Sabisch, X. Song, A. M. Minor, V. S. Battaglia and G. Liu, *Nano Lett.*, 2013, 13, 5397–5402.
22. J. S. Kim, W. Pfleging, R. Kohler, H. J. Seifert, T. Y. Kim, D. Byun, H.-G. Jung, W. Choi and J. K. Lee, *J. Power Sources*, 2015, 279, 13–20.

23. N.-S. Choi, K. H. Yew, K. Y. Lee, M. Sung, H. Kim and S.-S. Kim, *J. Power Sources*, 2006, 161, 1254–1259.
24. A. Magasinski, B. Zdyrko, I. Kovalenko, B. Hertzberg, R. Burtovyy, C. F. Huebner, T. F. Fuller, I. Luzinov and G. Yushin, *ACS Appl. Mater. Interfaces*, 2010, 2, 3004–3010.
25. I. Kovalenko, B. Zdyrko, A. Magasinski, B. Hertzberg, Z. Milicev, R. Burtovyy, I. Luzinov and G. Yushin, *Science*, 2011, 334, 75–79.
26. Swati Shrivastava et al., *Trends in Analytical Chemistry* 82 (2016) 55–67
27. Bao, z. et al., *Nature* 446, 172-175 (2007)
28. Ryu et al., *ACS Nano*, 2016, 10 (11) p. 10589-10597